General local energy-preserving integrators for solving multi-symplectic Hamiltonian PDEs

Yu–Wen Li[a], Xinyuan Wu[a,*]

[a]*Department of Mathematics, Nanjing University; State Key Laboratory for Novel Software Technology at Nanjing University, Nanjing 210093, P.R.China*

Abstract

In this paper we propose and investigate a general approach to constructing local energy-preserving algorithms which can be of arbitrarily high order in time for solving Hamiltonian PDEs. This approach is based on the temporal discretization using continuous Runge-Kutta-type methods, and the spatial discretization using pseudospectral methods or Gauss–Legendre collocation methods. The local energy conservation law of our new schemes is analyzed in detail. The effectiveness of the novel local energy-preserving integrators is demonstrated by coupled nonlinear Schrödinger equations and 2D nonlinear Schrödinger equations with external fields. Our new schemes are compared with some classical multi-symplectic and symplectic schemes in numerical experiments. The numerical results show the remarkable *long-term* behaviour of our new schemes.

Keywords: Multi-symplectic PDE, Local energy conservation law, Energy-preserving RK type method, Pseudospectral method, Gauss-Legendre collocation method, Local energy-preserving method

1. Introduction

Since the multi-symplectic structure was developed by Bridges and Marsden *et al.* [2, 27] for a class of PDEs, the construction and analysis of multi-symplectic numerical integrators which conserve the discrete multi-symplectic structure have become one of the central topics in PDE algorithms. Many multi-symplectic schemes have been proposed such as multi-symplectic RK/PRK/RKN methods, finite volume methods, spectral/ pseudospectral methods, splitting methods and wavelet collocation methods (see, e.g. [3, 4, 11, 18, 19, 26, 29, 30, 32]). All of these methods focus on the preservation of some kinds of discrete multi-symplecticity. However, multi-symplectic PDEs have many other important properties such as the local energy conservation law (ECL) and the local momentum conservation law (MCL). In general, multi-symplectic integrators can only preserve exactly quadratic conservation laws and invariants. In the paper [29], Reich firstly proposed two methods that preserve the discrete ECL and MCL respectively. In [31], Wang *et al.* generalized Reich's work. In [6, 7, 9], Chen *et al.*, and Cai *et al.* constructed some local structure-preserving schemes for special multi-symplectic PDEs. In [14], Gong *et al.* developed a general approach to constructing local structure-preserving algorithms. Local energy-preserving algorithms preserve the discrete global energy under suitable boundary conditions. Thus in the case of multi-symplectic PDEs, they cover the traditional global energy-preserving algorithms (see, e.g. [8, 13, 16, 21]). However, most of the local and global energy-preserving methods are based on the discrete gradient for the temporal discretization. Therefore, they can have only second order accuracy in time. We note that Hairer [17] developed a family of energy-preserving continuous Runge–Kutta–type

methods of arbitrarily high order for Hamiltonian ODEs. Motivated by Hairer's work, in this paper, we consider general local energy-preserving methods for multi-symplectic Hamiltonian PDEs, and we are hopeful of obtaining new high-order schemes which exactly preserve the ECL.

Besides, most of the existing local energy-preserving algorithms are based on the spatial discretization using the implicit midpoint rule. Although the authors in [8, 14] mentioned a class of global energy-preserving schemes based on the (pseudo) spectral discretization for the spatial derivative, it seems that there is little work investigating the local energy-preserving property of these schemes in the literature. In this paper, we investigate the preservation of the discrete ECL for our new schemes which are based on the pseudospectral spatial discretization. Meanwhile, we also design a class of local energy-preserving schemes based on the general Gauss-Legendre collocation spatial discretization.

The paper is organized as follows. In Section 2, we briefly introduce multi-symplectic PDEs and energy-preserving continuous Runge–Kutta methods. In Section 3, we present a general approach to constructing local energy-preserving schemes. This approach is illustrated by coupled nonlinear Schrödinger equations and 2D nonlinear Schrödinger equations in Section 4 and 5, respectively. We compare our new schemes with classical multi-symplectic and symplectic schemes in Section 6 and 7. The last section is concerned with the conclusion.

2. Multi-symplectic PDEs and energy-preserving continuous Runge–Kutta methods

A multi-symplectic PDE with one temporal variable and two spatial variables can be written in the form:

$$Mz_t + Kz_x + Lz_y = \nabla_z S(z), \quad z \in \mathbb{R}^d, \tag{1}$$

where M, K, and L are skew-symmetric d by d real matrices, $S : \mathbb{R}^d \to \mathbb{R}$ is a smooth scalar-valued function of the state variable variable z and ∇_z is the gradient operator. Three differential 2-forms are defined by

$$\omega = \frac{1}{2}dz \wedge Mdz, \quad \kappa = \frac{1}{2}dz \wedge Kdz, \quad \tau = \frac{1}{2}dz \wedge Ldz.$$

(1) then has the multi-symplectic conservation law (MSCL):

$$\partial_t \omega + \partial_x \kappa + \partial_y \tau = 0. \tag{2}$$

Another important local conservation law is the ECL:

$$\partial_t E + \partial_x F + \partial_y G = 0,$$

where

$$E = S(z) - \frac{1}{2}z^\mathsf{T} Kz_x - \frac{1}{2}z^\mathsf{T} Lz_y, \quad F = \frac{1}{2}z^\mathsf{T} Kz_t, \quad G = \frac{1}{2}z^\mathsf{T} Lz_t.$$

When $L = 0$, the equation (1) reduces to the case of one spatial dimension:

$$Mz_t + Kz_x = \nabla S(z). \tag{3}$$

Correspondingly, the ECL reduces to:

$$\partial_t E + \partial_x F = 0,$$

where

$$E = S(z) - \frac{1}{2}z^\mathsf{T} Kz_x, \quad F = \frac{1}{2}z^\mathsf{T} Kz_t.$$

Note that the energy density E is related to the gradient of S. If one is interested in constructing schemes which can preserve the discrete ECL, a natural idea is replacing ∇S by the discrete gradient (DG) $\bar{\nabla}S$. For details of the discrete gradient, readers are referred to [15, 25].

A limitation of the DG method is that it can only achieve second-order accuracy in general. Therefore, classical local energy-preserving methods based on the DG cannot reach an order higher than 2 in temporal direction unless the composition technique is applied, which is not our interest in this paper.

In contrast to the DG method, Hairer's seminal work overcomes the order barrier. In what follows, we introduce the approach summarily.

Consider autonomous ODEs:

$$\begin{cases} y' = f(y), \quad y \in \mathbb{R}^d, \\ y(t_0) = y_0. \end{cases} \tag{4}$$

Hairer's approach can be regarded as a continuous Runge–Kutta method :

$$\begin{cases} y_\tau = y_0 + h \int_0^1 A_{\tau,\sigma} f(y_\sigma) d\sigma, \\ y_1 = y_0 + h \int_0^1 B_\sigma f(y_\sigma) d\sigma, \\ B_\sigma \equiv 1, A_{\tau,\sigma} = \sum_{i=1}^s \frac{1}{b_i} \int_0^\tau l_i(\alpha) d\alpha \, l_i(\sigma), \end{cases} \tag{5}$$

where h is the stepsize, $\{l_i(\tau)\}_{i=1}^s$ are Lagrange interpolating polynomials based on the s distinct points $c_1, c_2, \ldots, c_s$, $b_i = \int_0^1 l_i(\tau) d\tau$ for $i = 1, 2, \ldots, s$, and y_τ approximates the value of $y(t_0 + \tau h)$ for $\tau \in [0, 1]$. The continuous RK method can be expressed in a Buchter tableau as

$$\begin{array}{c|c} C_\tau & A_{\tau,\sigma} \\ \hline & B_\tau \end{array}$$

with

$$\tau = C_\tau = \int_0^1 A_{\tau,\sigma} d\sigma.$$

If $f(y) = J^{-1} \nabla H(y)$, J is a skew-symmetric matrix, then this method preserves the Hamiltonian: $H(y_1) = H(y_0)$. Let r be the order of the quadrature formula $(b_i, c_i)_{i=1}^s$, then the order of this continuous method is given by:

$$\begin{cases} 2s, & \text{for } r \geq 2s - 1, \\ 2r - 2s + 2, & \text{for } r \leq 2s - 2. \end{cases} \tag{6}$$

Moreover, if the quadrature nodes are symmetric, i.e. $c_i = 1 - c_{s+1-i}$ for $i = 1, 2, \ldots, s$, then the method (5) is also symmetric. Clearly, by choosing an s-point Gauss-Legendre quadrature formula, we get a symmetric continuous RK method of order $2s$. Besides, although this method is not symplectic, it is conjugate-symplectic up to at least order $2s + 2$. The proof can be found in [17]. In view of these prominent properties, we select (5) as our elementary method for the time integration of Hamiltonian PDEs. We denote this method by CRK and call $(b_i, c_i)_{i=1}^s$ as the generating quadrature fomula in the remainder of this paper.

3. Construction of local energy-preserving algorithms for Hamiltonian PDEs

3.1. Pseudospectral spatial discretization

For simplicity, we first consider the following PDE with one spatial variable:

$$M z_t + K z_x = \nabla_z S(z, x). \tag{7}$$

In the classical multi-symplectic PDE (3), the Hamiltonian S is independent of the variable x. It should be noted that (7) does not have the MSCL and the MCL, but the local energy conservation law still holds:

$$\partial_t E + \partial_x F = 0, \tag{8}$$

where

$$E = S(z, x) - \frac{1}{2} z^\mathsf{T} K z_x, \quad F = \frac{1}{2} z^\mathsf{T} K z_t.$$

Thus local energy-preserving methods can be more widely used than classical multi-symplectic methods. Most of multi-symplectic methods can be constructed by concatenating two ODE methods in time and space, respectively.

The temporal method is always symplectic, while the spatial one may be not. However, in our new schemes, we use the CRK method instead of the symplectic method for the time integration. In this subsection, we consider a class of convenient methods for the spatial discretization under the periodic boundary condition. They are the Fourier spectral, the pseudospectral, and the wavelet collocation method (see, e.g. [4, 11, 32]). A common characteristic of the three methods is the substitution of a skew-symmetric differential matrix D for the operator ∂_x . For example, assuming $z(x_0, t) = z(x_0 + L, t)$, (7) becomes a system of ODEs in time after the pseudospectral spatial discretization :

$$M\frac{d}{dt}z_j + K\sum_{k=0}^{N-1} D_{jk}z_k = \nabla_z S(z_j, x_j), \tag{9}$$

for $j = 0, 1, \ldots, N - 1$, where N is an even integer, $x_j = x_0 + j\Delta x, j = 0, 1, \cdots, N - 1, \Delta x = \frac{L}{N}, z_j \approx z(x_j, t),$ D is a skew-symmetric matrix whose entries are determined by (see, e.g. [11])

$$D_{jk} = \begin{cases} \frac{\pi}{L}(-1)^{j+k}cot(\pi\frac{x_j - x_k}{L}), & j \neq k, \\ 0, & j = k. \end{cases}$$

Multiplying both sides of (9) by $\frac{d}{dt}z_j^\mathsf{T}$, we get N semi-discrete ECLs (see, e.g. [10, 23]):

$$\frac{d}{dt}E_j + \sum_{k=0}^{N-1} D_{jk}F_{jk} = 0, \tag{10}$$

for $j = 0, 1, \ldots, N - 1$, where

$$E_j = S(z_j, x_j) - \frac{1}{2}z_j^\mathsf{T} K\sum_{k=0}^{N-1} D_{jk}z_k,$$

$$F_{jk} = \frac{1}{2}z_k^\mathsf{T} K\frac{d}{dt}z_j + \frac{1}{2}z_j^\mathsf{T} K\frac{d}{dt}z_k.$$

The term $\sum_{k=0}^{N-1} D_{jk}F_{jk}$ can be considered as the discrete $\partial_x F(z_j)$:

$$\sum_{k=0}^{N-1} D_{jk}F_{jk} = \frac{1}{2}\delta_x z_j^\mathsf{T} K\frac{d}{dt}z_j + \frac{1}{2}z_j^\mathsf{T} K\frac{d}{dt}\delta_x z_j \approx \frac{1}{2}\partial_x z(x_j, t)^\mathsf{T} K\frac{d}{dt}z_j + \frac{1}{2}z_j^\mathsf{T} K\frac{d}{dt}\partial_x z(x_j, t) = \partial_x F(z_j), \tag{11}$$

where $\sum_{k=0}^{N-1} D_{jk}z_k = \delta_x z_j \approx \partial_x z(x_j, t)$.

If S is independent of the variable x, then N semi-discrete MSCLs (see, e.g. [4, 11]) also hold:

$$\frac{d}{dt}\omega_j + \sum_{k=0}^{N-1} D_{jk}\kappa_{jk} = 0,$$

$$\omega_j = \frac{1}{2}dz_j \wedge Mdz_j,$$

$$\kappa_{jk} = \frac{1}{2}(dz_j \wedge Kdz_k + dz_k \wedge Kdz_j),$$

for $j = 0, 1, \ldots, N - 1$. Here $\sum_{k=0}^{N-1} D_{jk}\kappa_{jk}$ (the discrete $\partial_x \kappa(z_j)$) can be comprehended in a similar way to (11).

After the temporal discretization using the CRK method (5), the full discrete scheme can be written as follows:

$$\begin{cases} z_j^\tau = z_j^0 + \Delta t \int_0^1 A_{\tau,\sigma}\delta_t z_j^\sigma d\sigma, \\ z_j^1 = z_j^0 + \Delta t \int_0^1 \delta_t z_j^\sigma d\sigma, \\ \delta_x z_j^\tau = \sum_{k=0}^{N-1} D_{jk}z_k^\tau, \\ M\delta_t z_j^\tau + K\delta_x z_j^\tau = \nabla_z S(z_j^\tau, x_j), \end{cases} \tag{12}$$

for $j = 0, 1, \ldots, N-1$, where $z_j^\tau \approx z(x_j, t_0 + \tau \Delta t)$, $\delta_t z_j^\tau \approx \partial_t z(x_j, t_0 + \tau \Delta t)$ are polynomials in τ. For the energy-preserving property of the CRK method, we expect this scheme to preserve some discrete ECLs. Firstly, note that $b_i = \int_0^1 l_i(\tau) d\tau$. For convenience, we denote

$$\frac{1}{b_i} \int_0^1 l_i(\tau) f(\tau) d\tau$$

(i.e. the weighted average of a function f with the weight function $l_i(\tau)$) as $\langle f \rangle_i$ in the remainder of our paper. Obviously, $\langle \cdot \rangle_i$ is a linear operator.

The next theorem shows the N-discrete local energy conservation law of (12).

Theorem 3.1. *The scheme* (12) *exactly conserves the N-discrete local energy conservation law:*

$$\frac{E_j^1 - E_j^0}{\Delta t} + \sum_{k=0}^{N-1} D_{jk} \bar{F}_{jk} = 0, \tag{13}$$

for $j = 0, 1, \ldots, N-1$, where

$$E_j^\alpha = S(z_j^\alpha, x_j) - \frac{1}{2} z_j^{\alpha\mathsf{T}} K \delta_x z_j^\alpha, \, \alpha = 0, 1,$$

$$\bar{F}_{jk} = \frac{1}{2} \sum_{i=1}^{s} b_i (\langle z_j \rangle_i^\mathsf{T} K \langle \delta_t z_k \rangle_i + \langle z_k \rangle_i^\mathsf{T} K \langle \delta_t z_j \rangle_i).$$

By summing the identities (13) from $j = 0$ to $N-1$, on noticing that $\bar{F}_{jk}$ is symmetric with respect to j, k and D_{jk} is anti-symmetric with respect to j, k, the discrete ECLs lead to the global energy conservation:

$$\Delta x \sum_{j=0}^{N-1} E_j^1 - \Delta x \sum_{j=0}^{N-1} E_j^0 = -\Delta x \Delta t \sum_{j=0}^{N-1} \sum_{k=0}^{N-1} D_{jk} \bar{F}_{jk} = 0. \tag{14}$$

If we evaluate the integrals of $\bar{F}_{jk}$ by the generating quadrature formula of the CRK method, we have

$$\bar{F}_{jk} \approx \frac{1}{2} \sum_{i=1}^{s} b_i (z_j^{c_i\mathsf{T}} K \delta_t z_k^{c_i} + z_k^{c_i\mathsf{T}} K \delta_t z_j^{c_i}).$$

Proof. First of all, note that the discrete differential operator δ_x is linear, thus it holds that

$$\partial_\tau \delta_x z_j^\tau = \delta_x \partial_\tau z_j^\tau. \tag{15}$$

It follows from (12) that

$$\partial_\tau z_j^\tau = \Delta t \int_0^1 \sum_{i=1}^{s} \frac{1}{b_i} l_i(\tau) l_i(\sigma) \delta_t z_j^\sigma d\sigma = \Delta t \sum_{i=1}^{s} l_i(\tau) \langle \delta_t z_j \rangle_i. \tag{16}$$

Then we have

$$S(z_j^1, x_j) - S(z_j^0, x_j)$$
$$= \int_0^1 \partial_\tau z_j^{\tau\mathsf{T}} \nabla_z S(z_j^\tau, x_j) d\tau = \Delta t \sum_{i=1}^{s} b_i \langle \delta_t z_j \rangle_i^\mathsf{T} \langle \nabla_z S_j \rangle_i, \tag{17}$$

$$z_j^1 K \delta_x z_j^1 - z_j^0 K \delta_x z_j^0$$
$$= \int_0^1 \partial_\tau (z_j^{\tau\mathsf{T}} K \delta_x z_j^\tau) d\tau = \int_0^1 (\partial_\tau z_j^{\tau\mathsf{T}} K \delta_x z_j^\tau + z_j^{\tau\mathsf{T}} K \delta_x \partial_\tau z_j^\tau) d\tau$$
$$= \Delta t \sum_{i=1}^{s} b_i \langle \delta_t z_j \rangle_i^\mathsf{T} K \langle \delta_x z_j \rangle_i + \Delta t \sum_{i=1}^{s} b_i \langle z_j \rangle_i^\mathsf{T} K \langle \delta_x \delta_t z_j \rangle_i. \tag{18}$$

With (17) and (18), it follows from

$$\mathbf{a}^\mathsf{T} M \mathbf{a} = 0, \quad \mathbf{a}^\mathsf{T} M \mathbf{b} = -\mathbf{b}^\mathsf{T} M \mathbf{a}$$

that, for $\mathbf{a}, \mathbf{b} \in \mathbb{R}^d$, we have

$$
\begin{aligned}
(E_j^1 &- E_j^0)/\Delta t \\
&= (S(z_j^1, x_j) - S(z_j^0, x_j) - \frac{1}{2}(z_j^{1\mathsf{T}} K \delta_x z_j^1 - z_j^{0\mathsf{T}} K \delta_x z_j^0))/\Delta t \\
&= \sum_{i=1}^{s} b_i \langle \delta_t z_j \rangle_i^{\mathsf{T}} \langle M \delta_t z_j + K \delta_x z_j \rangle_i - \frac{1}{2} \sum_{i=1}^{s} b_i \langle \delta_t z_j \rangle_i^{\mathsf{T}} K \langle \delta_x z_j \rangle_i - \frac{1}{2} \sum_{i=1}^{s} b_i \langle z_j \rangle_i^{\mathsf{T}} K \langle \delta_x \delta_t z_j \rangle_i \\
&= \frac{1}{2} \sum_{i=1}^{s} b_i \langle \delta_t z_j \rangle_i^{\mathsf{T}} K \langle \delta_x z_j \rangle_i - \frac{1}{2} \sum_{i=1}^{s} b_i \langle z_j \rangle_i^{\mathsf{T}} K \langle \delta_x \delta_t z_j \rangle_i \\
&= \frac{1}{2} \sum_{k=0}^{N-1} D_{jk} \sum_{i=1}^{s} b_i \langle \delta_t z_j \rangle_i^{\mathsf{T}} K \langle z_k \rangle_i - \frac{1}{2} \sum_{k=0}^{N-1} D_{jk} \sum_{i=1}^{s} b_i \langle z_j \rangle_i^{\mathsf{T}} K \langle \delta_t z_k \rangle_i \\
&= - \sum_{k=0}^{N-1} D_{jk} \bar{F}_{jk}
\end{aligned}
\tag{19}
$$

$\square$

Note that a crucial property of the pseudospectral method is replacing the operator ∂_x with a linear and skew-symmetric differential matrix. Fortunately, this property is shared by spectral methods and wavelet collocation methods, hence our procedure of constructing the local energy-preserving scheme can be applied to them without any trouble.

Our approach can also be easily generalized to high dimensional problems. For example, we consider the following equation :

$$
M z_t + K z_x + L z_y = \nabla_z S(z, x, y). \tag{20}
$$

The ECL of this equation is:

$$
\partial_t E + \partial_x F + \partial_y G = 0, \tag{21}
$$

where

$$
E = S(z, x, y) - \frac{1}{2} z^{\mathsf{T}} K z_x - \frac{1}{2} z^{\mathsf{T}} L z_y, \quad F = \frac{1}{2} z^{\mathsf{T}} K z_t, \quad G = \frac{1}{2} z^{\mathsf{T}} L z_t.
$$

Applying a CRK method to t-direction and a pseudospectral method to x and y directions (under the periodic boundary condition $z(x_0, y, t) = z(x_0 + L_1, y, t), z(x, y_0, t) = z(x, y_0 + L_2, t)$) gives the following full discrete scheme:

$$
\begin{cases}
z_{jl}^{\tau} = z_{jl}^0 + \Delta t \int_0^1 A_{\tau,\sigma} \delta_t z_{jl}^{\sigma} d\sigma, \\[2mm]
z_{jl}^1 = z_{jl}^0 + \Delta t \int_0^1 \delta_t z_{jl}^{\sigma} d\sigma, \\[2mm]
\delta_x z_{jl}^{\tau} = \sum_{k=0}^{N-1} (D_x)_{jk} z_{kl}^{\tau}, \\[2mm]
\delta_y z_{jl}^{\tau} = \sum_{m=0}^{M-1} (D_y)_{lm} z_{jm}^{\tau}, \\[2mm]
M \delta_t z_{jl}^{\tau} + K \delta_x z_{jl}^{\tau} + L \delta_y z_{jl}^{\tau} = \nabla_z S(z_{jl}^{\tau}, x_j, y_l),
\end{cases}
\tag{22}
$$

for $j = 0, 1, \ldots, N-1$, $l = 0, 1, \ldots, M-1$, where $z_{jl}^{\tau} \approx z(x_j, y_l, t_0 + \tau \Delta t)$, $\delta_t z_{jl}^{\tau} \approx \partial_t z(x_j, y_l, t_0 + \tau \Delta t)$ are polynomials in τ, $x_j = x_0 + j\Delta x$, $y_l = y_0 + l\Delta y$, $\Delta x = \frac{L_1}{N}$, $\Delta y = \frac{L_2}{M}$. Both D_x and D_y are pseudospectral differential matrices related to x and y directions respectively.

The next theorem presents the discrete local energy conservation laws of (22).

Theorem 3.2. *The scheme* (22) *exactly conserves the NM-discrete local energy conservation law:*

$$
\frac{E_{jl}^1 - E_{jl}^0}{\Delta t} + \sum_{k=0}^{N-1} (D_x)_{jk} \bar{F}_{jk,l} + \sum_{m=0}^{M-1} (D_y)_{lm} \bar{G}_{j,lm} = 0, \tag{23}
$$

for $j = 0, 1, \ldots, N - 1, \quad l = 0, 1, \ldots, M - 1,$ *where*

$$E_j^\alpha = S(z_{jl}^\alpha, x_j, y_l) - \frac{1}{2} z_{jl}^{\alpha\mathsf{T}} K \delta_x z_{jl}^\alpha - \frac{1}{2} z_{jl}^{\alpha\mathsf{T}} L \delta_y z_{jl}^\alpha, \alpha = 0, 1,$$

$$\bar{F}_{jk,l} = \frac{1}{2} \sum_{i=1}^s b_i (\langle z_{jl} \rangle_i^\mathsf{T} K \langle \delta_t z_{kl} \rangle_i + \langle z_{kl} \rangle_i^\mathsf{T} K \langle \delta_t z_{jl} \rangle_i),$$

$$\bar{G}_{j,lm} = \frac{1}{2} \sum_{i=1}^s b_i (\langle z_{jl} \rangle_i^\mathsf{T} L \langle \delta_t z_{jm} \rangle_i + \langle z_{jm} \rangle_i^\mathsf{T} L \langle \delta_t z_{jl} \rangle_i).$$

Since the proof of Theorem 3.2 is very similar to that of Theorem 3.1, we omit the details here.

Summing the identities (23) over all space grid points, on noticing that $\bar{F}_{jk,l}$ is symmetric with respect to j, k, and $(D_x)_{jk}$ is anti-symmetric with respect to j, k, $\bar{G}_{j,lm}$ is symmetric with respect to l, m, and $(D_y)_{lm}$ is anti-symmetric with respect to l, m, again, we obtain the global energy conservation :

$$\Delta x \Delta y \sum_{j=0}^{N-1} \sum_{l=0}^{M-1} E_{jl}^1 - \Delta x \Delta y \sum_{j=0}^{N-1} \sum_{l=0}^{M-1} E_{jl}^0 = -\Delta t \Delta x \Delta y \sum_{j=0}^{N-1} \sum_{l=0}^{M-1} \sum_{k=0}^{N-1} (D_x)_{jk} \bar{F}_{jk,l} - \Delta t \Delta x \Delta y \sum_{j=0}^{N-1} \sum_{l=0}^{M-1} \sum_{m=0}^{M-1} (D_y)_{lm} \bar{G}_{j,lm} = 0. \quad (24)$$

3.2. *Gauss-Legendre collocation spatial discretization*

In multi-symplectic algorithms, another class of methods frequently applied to spatial discretization is the Gauss-Legendre (GL) collocation method. We assume that the Butcher tableau of the GL method is:

$$
\begin{array}{c|ccc}
\tilde{c}_1 & \tilde{a}_{11} & \cdots & \tilde{a}_{1r} \\
\vdots & \vdots & \ddots & \vdots \\
\tilde{c}_r & \tilde{a}_{r1} & \cdots & \tilde{a}_{rr} \\
\hline
& \tilde{b}_1 & \cdots & \tilde{b}_r
\end{array}
\quad (25)
$$

After the spatial discretization using the GL method (25) and the temporal discretization using the CRK, we obtain the full discrete scheme of (7) :

$$
\begin{cases}
z_{n,j}^\tau = z_{n,j}^0 + \Delta t \int_0^1 A_{\tau,\sigma} \delta_t z_{n,j}^\sigma d\sigma, \\[2mm]
z_{n,j}^1 = z_{n,j}^0 + \Delta t \int_0^1 \delta_t z_{n,j}^\sigma d\sigma, \\[2mm]
z_{n,j}^\tau = z_n^\tau + \Delta x \sum_{k=1}^r \tilde{a}_{jk} \delta_x z_{n,k}^\tau, \\[2mm]
z_{n+1}^\tau = z_n^\tau + \Delta x \sum_{j=1}^r \tilde{b}_j \delta_x z_{n,j}^\tau, \\[2mm]
M \delta_t z_{n,j}^\tau + K \delta_x z_{n,j}^\tau = \nabla_z S(z_{n,j}^\tau, x_n + \tilde{c}_j \Delta x),
\end{cases}
\quad (26)
$$

for $j = 1, 2, \ldots, r$, where $z_n^\tau \approx z(x_n, t_0 + \tau \Delta t), z_{n+1}^\tau \approx z(x_n + \Delta x, t_0 + \tau \Delta t), z_{n,j}^\tau \approx z(x_n + \tilde{c}_j \Delta x, t_0 + \tau \Delta t), \delta_t z_{n,j}^\tau \approx \partial_t z(x_n + \tilde{c}_j \Delta x, t_0 + \tau \Delta t), \delta_x z_{n,j}^\tau \approx \partial_x z(x_n + \tilde{c}_j \Delta x, t_0 + \tau \Delta t)$ are polynomials in τ. This is a local scheme on the box $[x_n, x_n + \Delta x] \times [t_0, t_0 + \Delta t]$. To show that (26) exactly conserves the discrete ECL, we should make sure that there is some law of commutation between δ_t and δ_x. To this end we introduce the following auxiliary system:

$$
\begin{aligned}
\delta_x z_{n,j}^\tau &= \delta_x z_{n,j}^0 + \Delta t \int_0^1 A_{\tau,\sigma} \delta_t \delta_x z_{n,j}^\sigma d\sigma, \\[2mm]
\delta_x z_{n,j}^1 &= \delta_x z_{n,j}^0 + \Delta t \int_0^1 \delta_t \delta_x z_{n,j}^\sigma d\sigma, \\[2mm]
\delta_t z_{n,j}^\tau &= \delta_t z_n^\tau + \Delta x \sum_{k=1}^r \tilde{a}_{jk} \delta_x \delta_t z_{n,k}^\tau, \\[2mm]
\delta_t z_{n+1}^\tau &= \delta_t z_n^\tau + \Delta x \sum_{j=1}^r \tilde{b}_j \delta_x \delta_t z_{n,j}^\tau,
\end{aligned}
\quad (27)
$$

for $j = 1, 2, \ldots, r$, where $\delta_t \delta_x z_{n,j}^\sigma \approx \partial_t \partial_x z(x_n + \tilde{c}_j \Delta x, t_0 + \sigma t)$, $\delta_x \delta_t z_{n,j}^\sigma \approx \partial_x \partial_t z(x_n + \tilde{c}_j \Delta x, t_0 + \sigma t)$. Then

$$
\begin{aligned}
z_{n,j}^\tau &= z_{n,j}^0 + \Delta t \int_0^1 A_{\tau,\sigma} \delta_t z_{n,j}^\sigma d\sigma \\
&= z_{n,j}^0 + \Delta t \int_0^1 A_{\tau,\sigma}(\delta_t z_n^\sigma + \Delta x \sum_{k=1}^r \tilde{a}_{jk} \delta_x \delta_t z_{n,k}^\sigma)d\sigma \\
&= z_{n,j}^0 + z_n^\tau - z_n^0 + \Delta t \Delta x \sum_{k=1}^r \tilde{a}_{jk} \int_0^1 A_{\tau,\sigma} \delta_x \delta_t z_{n,k}^\sigma d\sigma.
\end{aligned}
\tag{28}
$$

Likewise,

$$
z_{n,j}^\tau = z_n^\tau + z_{n,j}^0 - z_n^0 + \Delta x \Delta t \sum_{k=1}^r \tilde{a}_{jk} \int_0^1 A_{\tau,\sigma} \delta_t \delta_x z_{n,k}^\sigma d\sigma.
\tag{29}
$$

(28), (29) lead to

$$
\sum_{k=1}^r \tilde{a}_{jk} \int_0^1 A_{\tau,\sigma} \delta_x \delta_t z_{n,k}^\sigma d\sigma = \sum_{k=1}^r \tilde{a}_{jk} \int_0^1 A_{\tau,\sigma} \delta_t \delta_x z_{n,k}^\sigma d\sigma.
$$

Since the matrix $(\tilde{a}_{jk})_{1 \le j, k \le r}$ is invertible, we have

$$
\int_0^1 A_{\tau,\sigma} \delta_x \delta_t z_{n,k}^\sigma d\sigma = \int_0^1 A_{\tau,\sigma} \delta_t \delta_x z_{n,k}^\sigma d\sigma, \quad \tau \in [0, 1],
\tag{30}
$$

for $k = 1, 2, \ldots, r$. Taking derivatives with respect to τ on both sides of (30), we arrive at

$$
\int_0^1 (\sum_{i=1}^s \frac{1}{b_i} l_i(\tau) l_i(\sigma)) \delta_x \delta_t z_{n,k}^\sigma d\sigma = \int_0^1 (\sum_{i=1}^s \frac{1}{b_i} l_i(\tau) l_i(\sigma)) \delta_t \delta_x z_{n,k}^\sigma d\sigma, \quad \tau \in [0, 1],
$$

for $k = 1, 2, \ldots, r$. Finally, setting $\tau = c_1, \ldots, c_s$, we have the following lemma:

Lemma 3.3. *The following discrete commutability between δ_t and δ_x holds:*

$$
\langle \delta_x \delta_t z_{n,j} \rangle_i = \langle \delta_t \delta_x z_{n,j} \rangle_i,
\tag{31}
$$

for $i = 1, \ldots, s, \quad j = 1, 2, \ldots, r$.

Theorem 3.4. *The scheme* (26) *conserves the following discrete local energy conservation law :*

$$
\Delta x \sum_{j=1}^r \tilde{b}_j (E_{n,j}^1 - E_{n,j}^0) + \Delta t (\bar{F}_{n+1} - \bar{F}_n) = 0,
\tag{32}
$$

where

$$
E_{n,j}^\alpha = S(z_{n,j}^\alpha, x_n + \tilde{c}_j \Delta x) - \frac{1}{2} z_{n,j}^{\alpha \mathsf{T}} K \delta_x z_{n,j}^\alpha, \alpha = 0, 1,
$$

$$
\bar{F}_\beta = \frac{1}{2} \sum_{i=1}^s b_i \langle z_\beta \rangle_i^\mathsf{T} K \langle \delta_t z_\beta \rangle_i, \beta = n, n+1.
$$

Proof. It follows from the first equation of (26) that,

$$
\partial_\tau z_{n,j}^\tau = \Delta t \sum_{i=1}^s l_i(\tau) \langle \delta_t z_{n,j} \rangle_i.
\tag{33}
$$

The result in the temporal direction is almost the same as the pseudospectral case :

$$
S(z_{n,j}^1, x_n + \tilde{c}_j \Delta x) - S(z_{n,j}^0, x_n + \tilde{c}_j \Delta x) = \Delta t \sum_{i=1}^s b_i \langle \delta_t z_{n,j} \rangle_i^\mathsf{T} \langle \nabla S_{n,j} \rangle_i,
$$

$$z_{n,j}^1 K \delta_x z_{n,j}^1 - z_{n,j}^0 K \delta_x z_{n,j}^0 = \Delta t \sum_{i=1}^{s} b_i \langle \delta_t z_{n,j} \rangle_i^\mathsf{T} K \langle \delta_x z_{n,j} \rangle_i + \Delta t \sum_{i=1}^{s} b_i \langle z_{n,j} \rangle_i^\mathsf{T} K \langle \delta_t \delta_x z_{n,j} \rangle_i.$$

Hence

$$
\begin{aligned}
& E_{n,j}^1 - E_{n,j}^0 \\
&= S(z_{n,j}^1, x_n + \tilde{c}_j \Delta x) - S(z_{n,j}^0, x_n + \tilde{c}_j \Delta x) - \frac{1}{2}(z_{n,j}^1 K \delta_x z_{n,j}^1 - z_{n,j}^0 K \delta_x z_{n,j}^0) \\
&= \Delta t \sum_{i=1}^{s} b_i \langle \delta_t z_{n,j} \rangle_i^\mathsf{T} \langle M \delta_t z_{n,j} + K \delta_x z_{n,j} \rangle_i - \frac{1}{2}\Delta t \sum_{i=1}^{s} b_i \langle \delta_t z_{n,j} \rangle_i^\mathsf{T} K \langle \delta_x z_{n,j} \rangle_i - \frac{1}{2}\Delta t \sum_{i=1}^{s} b_i \langle z_{n,j} \rangle_i^\mathsf{T} K \langle \delta_t \delta_x z_{n,j} \rangle_i \\
&= \frac{1}{2}\Delta t \sum_{i=1}^{s} b_i \langle \delta_t z_{n,j} \rangle_i^\mathsf{T} K \langle \delta_x z_{n,j} \rangle_i - \frac{1}{2}\Delta t \sum_{i=1}^{s} b_i \langle z_{n,j} \rangle_i^\mathsf{T} K \langle \delta_t \delta_x z_{n,j} \rangle_i.
\end{aligned}
\tag{34}
$$

On the other hand,

$$
\begin{aligned}
& z_{n+1}^{\tau\mathsf{T}} K \delta_t z_{n+1}^\sigma - z_n^{\tau\mathsf{T}} K \delta_t z_n^\sigma \\
&= (z_n^{\tau\mathsf{T}} + \Delta x \sum_{j=1}^{r} \tilde{b}_j \delta_x z_{n,j}^{\tau\mathsf{T}}) K (\delta_t z_n^\sigma + \Delta x \sum_{j=1}^{r} \tilde{b}_j \delta_x \delta_t z_{n,j}^\sigma) - z_n^{\tau\mathsf{T}} K \delta_t z_n^\sigma \\
&= \Delta x \sum_{j=1}^{r} \tilde{b}_j z_n^{\tau\mathsf{T}} K \delta_x \delta_t z_{n,j}^\sigma + \Delta x \sum_{j=1}^{r} \tilde{b}_j \delta_x z_{n,j}^{\tau\mathsf{T}} K \delta_t z_n^\sigma + \Delta x^2 \sum_{j,k=1}^{r} \tilde{b}_j \tilde{b}_k \delta_x z_{n,j}^{\tau\mathsf{T}} K \delta_x \delta_t z_{n,k}^\sigma \\
&= \Delta x \sum_{j=1}^{r} \tilde{b}_j (z_{n,j}^{\tau\mathsf{T}} - \Delta x \sum_{k=1}^{r} \tilde{a}_{jk} \delta_x z_{n,k}^{\tau\mathsf{T}}) K \delta_x \delta_t z_{n,j}^\sigma + \Delta x \sum_{j=1}^{r} \tilde{b}_j \delta_x z_{n,j}^{\tau\mathsf{T}} K (\delta_t z_{n,j}^\sigma - \Delta x \sum_{k=1}^{r} \tilde{a}_{jk} \delta_x \delta_t z_{n,k}^\sigma) \\
&\quad + \Delta x^2 \sum_{j,k=1}^{r} \tilde{b}_j \tilde{b}_k \delta_x z_{n,j}^{\tau\mathsf{T}} K \delta_x \delta_t z_{n,k}^\sigma \\
&= \Delta x \sum_{j=1}^{r} \tilde{b}_j z_{n,j}^{\tau\mathsf{T}} K \delta_x \delta_t z_{n,j}^\sigma + \Delta x \sum_{j=1}^{r} \tilde{b}_j \delta_x z_{n,j}^{\tau\mathsf{T}} K \delta_t z_{n,j}^\sigma + \Delta x^2 \sum_{j,k=1}^{r} (\tilde{b}_j \tilde{b}_k - \tilde{b}_j \tilde{a}_{jk} - \tilde{b}_k \tilde{a}_{kj}) \delta_x z_{n,j}^{\tau\mathsf{T}} K \delta_x \delta_t z_{n,k}^\sigma \\
&= \Delta x \sum_{j=1}^{r} \tilde{b}_j z_{n,j}^{\tau\mathsf{T}} K \delta_x \delta_t z_{n,j}^\sigma + \Delta x \sum_{j=1}^{r} \tilde{b}_j \delta_x z_{n,j}^{\tau\mathsf{T}} K \delta_t z_{n,j}^\sigma.
\end{aligned}
\tag{35}
$$

It follows from (35) that

$$
\begin{aligned}
& \bar{F}_{n+1} - \bar{F}_n \\
&= \frac{1}{2} \sum_{i=1}^{s} b_i (\langle z_{n+1} \rangle_i^\mathsf{T} K \langle \delta_t z_{n+1} \rangle_i - \langle z_n \rangle_i^\mathsf{T} K \langle \delta_t z_n \rangle_i) \\
&= \frac{1}{2}\Delta x \sum_{j=1}^{r} \sum_{i=1}^{s} \tilde{b}_j b_i (\langle z_{n,j} \rangle_i^\mathsf{T} K \langle \delta_x \delta_t z_{n,j} \rangle_i + \langle \delta_x z_{n,j} \rangle_i^\mathsf{T} K \langle \delta_t z_{n,j} \rangle_i)
\end{aligned}
\tag{36}
$$

From (34) and (36), using Lemma 3.3, we have

$$
\begin{aligned}
& \Delta x \sum_{j=1}^{r} \tilde{b}_j (E_{n,j}^1 - E_{n,j}^0) + \Delta t(\bar{F}_{n+1} - \bar{F}_n) \\
&= \frac{1}{2}\Delta t \Delta x \sum_{i=1}^{s} \sum_{j=1}^{r} \tilde{b}_j b_i (\langle \delta_t z_{n,j} \rangle_i^\mathsf{T} K \langle \delta_x z_{n,j} \rangle_i - \langle z_{n,j} \rangle_i^\mathsf{T} K \langle \delta_t \delta_x z_{n,j} \rangle_i + \langle z_{n,j} \rangle_i^\mathsf{T} K \langle \delta_x \delta_t z_{n,j} \rangle_i + \langle \delta_x z_{n,j} \rangle_i^\mathsf{T} K \langle \delta_t z_{n,j} \rangle_i) \\
&= \frac{1}{2}\Delta x \Delta t \sum_{j=1}^{r} \sum_{i=1}^{s} \tilde{b}_j b_i \langle z_{n,j} \rangle_i^\mathsf{T} K (\langle \delta_x \delta_t z_{n,j} \rangle_i - \langle \delta_t \delta_x z_{n,j} \rangle_i) = 0.
\end{aligned}
\tag{37}
$$

□

Assume that the spatial domain is divided equally into N intervals and the corresponding grids are $x_0, x_1, \ldots, x_N$. By summing the identities (32) from $n = 0$ to $N - 1$, we obtain the global energy conservation of the scheme (26) under the periodic boundary condition :

$$\Delta x \sum_{n=0}^{N-1} \sum_{j=1}^{r} \tilde{b}_j E_{n,j}^1 - \Delta x \sum_{n=0}^{N-1} \sum_{j=1}^{r} \tilde{b}_j E_{n,j}^0 = -\Delta t \sum_{n=0}^{N-1} (\bar{F}_{n+1} - \bar{F}_n) = 0, \tag{38}$$

The GL spatial discretization is not restricted to the periodic boundary condition (PBC). Thus the discrete ECL (32) is superior to the discrete global energy conservation (38). However, discretizing space by high-order GL methods may lead to singular and massive ODE systems which are expensive to solve (see, e.g. [26, 30]). For this reason, we will not include the scheme (26) in our numerical experiments in Section 6, 7.

4. Local energy-preserving schemes for coupled nonlinear Schrödinger equations

An important class of multi-symplectic PDEs is the (coupled) nonlinear Schrödinger equation ((C)NLS). A great number of them have polynomial nonlinear terms, hence we can calculate the integrals exactly in our method (for example, by symbol calculations). Here we summarily introduce the multi-symplectic structure of the 2-coupled NLS:

$$\begin{cases} iu_t + i\alpha u_x + \dfrac{1}{2}u_{xx} + (|u|^2 + \beta|v|^2)u = 0, \\ iv_t - i\alpha v_x + \dfrac{1}{2}v_{xx} + (\beta|u|^2 + |v|^2)v = 0, \end{cases} \tag{39}$$

where u, v are complex variables, i is the imaginary unit. Assuming $u = q_1 + iq_2$ and $v = q_3 + iq_4$, $\partial_x q_i = 2p_i$, q_i are real variables for $i = 1, 2, 3, 4$, we can formulate this equation to a multi-symplectic form (see, e.g. [10]):

$$\begin{pmatrix} \mathbf{J}_1 & \mathbf{O} \\ \mathbf{O} & \mathbf{O} \end{pmatrix} z_t + \begin{pmatrix} \mathbf{J}_2 & \mathbf{I} \\ -\mathbf{I} & \mathbf{O} \end{pmatrix} z_x = \nabla S(z),$$

where

$$\mathbf{J}_1 = \begin{pmatrix} 0 & -1 & 0 & 0 \\ 1 & 0 & 0 & 0 \\ 0 & 0 & 0 & -1 \\ 0 & 0 & 1 & 0 \end{pmatrix}, \mathbf{J}_2 = \begin{pmatrix} 0 & -\alpha & 0 & 0 \\ \alpha & 0 & 0 & 0 \\ 0 & 0 & 0 & \alpha \\ 0 & 0 & -\alpha & 0 \end{pmatrix}, \mathbf{O} = \begin{pmatrix} 0 & 0 & 0 & 0 \\ 0 & 0 & 0 & 0 \\ 0 & 0 & 0 & 0 \\ 0 & 0 & 0 & 0 \end{pmatrix}, \mathbf{I} = \begin{pmatrix} 1 & 0 & 0 & 0 \\ 0 & 1 & 0 & 0 \\ 0 & 0 & 1 & 0 \\ 0 & 0 & 0 & 1 \end{pmatrix},$$

and

$$z = (q_1, q_2, q_3, q_4, p_1, p_2, p_3, p_4)^\top, \quad S = -\frac{1}{4}(q_1^2 + q_2^2)^2 - \frac{1}{4}(q_3^2 + q_4^2)^2 - \frac{1}{2}\beta(q_1^2 + q_2^2)(q_3^2 + q_4^2) - (p_1^2 + p_2^2 + p_3^2 + p_4^2).$$

The corresponding energy density E and flux F in the ECL (8) are:

$$E = S - \alpha(q_2 p_1 - q_1 p_2 + q_3 p_4 - q_4 p_3) - \frac{1}{2}\sum_{i=1}^{4}(q_i \partial_x p_i - 2p_i^2),$$

$$F = \frac{1}{2}(\alpha(q_2 \partial_t q_1 - q_1 \partial_t q_2 + q_3 \partial_t q_4 - q_4 \partial_t q_3) + \sum_{i=1}^{4}(q_i \partial_t p_i - p_i \partial_t q_i)).$$

The corresponding MCL of this equation is:

$$\partial_t I + \partial_x G = 0,$$

where

$$I = q_2 p_1 - q_1 p_2 + q_4 p_3 - q_3 p_4,$$

$$G = S - \frac{1}{2}(q_2 \partial_t q_1 - q_1 \partial_t q_2 + q_4 \partial_t q_3 - q_3 \partial_t q_4).$$

Integrating the ECL and MCL with respect to the variable x under the PBC leads to the global energy and the momentum conservation:

$$\int_{x_0}^{x_0+L} E(x,t)dx = \int_{x_0}^{x_0+L} E(x,0)dx, \quad \int_{x_0}^{x_0+L} I(x,t)dx = \int_{x_0}^{x_0+L} I(x,0)dx.$$

Besides, the global charges of u and v are constant under the PBC:

$$\int_{x_0}^{x_0+L} |u(x,t)|^2 dx = \int_{x_0}^{x_0+L} |u(x,0)|^2 dx, \quad \int_{x_0}^{x_0+L} |v(x,t)|^2 dx = \int_{x_0}^{x_0+L} |v(x,0)|^2 dx.$$

Applying our discrete procedure to the equation (39) gives the following scheme in vector form:

$$
\begin{cases}
q_1^\tau = q_1^0 + \Delta t \int_0^1 A_{\tau,\sigma}(-\alpha Dq_1^\sigma - Dp_2^\sigma - (((q_1^\sigma)^{\cdot 2} + (q_2^\sigma)^{\cdot 2}) + \beta((q_3^\sigma)^{\cdot 2} + (q_4^\sigma)^{\cdot 2})) \cdot q_2^\sigma)d\sigma, \\[2mm]
q_2^\tau = q_2^0 + \Delta t \int_0^1 A_{\tau,\sigma}(-\alpha Dq_2^\sigma + Dp_1^\sigma + (((q_1^\sigma)^{\cdot 2} + (q_2^\sigma)^{\cdot 2}) + \beta((q_3^\sigma)^{\cdot 2} + (q_4^\sigma)^{\cdot 2})) \cdot q_1^\sigma)d\sigma, \\[2mm]
q_3^\tau = q_3^0 + \Delta t \int_0^1 A_{\tau,\sigma}(\alpha Dq_3^\sigma - Dp_4^\sigma - (\beta((q_1^\sigma)^{\cdot 2} + (q_2^\sigma)^{\cdot 2}) + ((q_3^\sigma)^{\cdot 2} + (q_4^\sigma)^{\cdot 2})) \cdot q_4^\sigma)d\sigma, \\[2mm]
q_4^\tau = q_4^0 + \Delta t \int_0^1 A_{\tau,\sigma}(\alpha Dq_4^\sigma + Dp_3^\sigma + (\beta((q_1^\sigma)^{\cdot 2} + (q_2^\sigma)^{\cdot 2}) + ((q_3^\sigma)^{\cdot 2} + (q_4^\sigma)^{\cdot 2})) \cdot q_3^\sigma)d\sigma, \\[2mm]
q_1^1 = q_1^0 + \Delta t \int_0^1 (-\alpha Dq_1^\sigma - Dp_2^\sigma - (((q_1^\sigma)^{\cdot 2} + (q_2^\sigma)^{\cdot 2}) + \beta((q_3^\sigma)^{\cdot 2} + (q_4^\sigma)^{\cdot 2})) \cdot q_2^\sigma)d\sigma, \\[2mm]
q_2^1 = q_2^0 + \Delta t \int_0^1 (-\alpha Dq_2^\sigma + Dp_{1,k}^\sigma + (((q_1^\sigma)^{\cdot 2} + (q_2^\sigma)^{\cdot 2}) + \beta((q_3^\sigma)^{\cdot 2} + (q_4^\sigma)^{\cdot 2})) \cdot q_1^\sigma)d\sigma, \\[2mm]
q_3^1 = q_3^0 + \Delta t \int_0^1 (\alpha Dq_3^\sigma - Dp_4^\sigma - (\beta((q_1^\sigma)^{\cdot 2} + (q_2^\sigma)^{\cdot 2}) + ((q_3^\sigma)^{\cdot 2} + (q_4^\sigma)^{\cdot 2})) \cdot q_4^\sigma)d\sigma, \\[2mm]
q_4^1 = q_4^0 + \Delta t \int_0^1 (\alpha Dq_4^\sigma + Dp_3^\sigma + (\beta((q_1^\sigma)^{\cdot 2} + (q_2^\sigma)^{\cdot 2}) + ((q_3^\sigma)^{\cdot 2} + (q_4^\sigma)^{\cdot 2})) \cdot q_3^\sigma)d\sigma, \\[2mm]
\delta_x q_i^\sigma = Dq_i^\sigma = 2p_i^\sigma, \ i = 1,2,3,4,
\end{cases}
\tag{40}
$$

where $q_i^a = (q_{i,0}^a, q_{i,1}^a, \ldots, q_{i,N-1}^a)^\mathsf{T}$, $p_i^a = (p_{i,0}^a, p_{i,1}^a, \ldots, p_{i,N-1}^a)^\mathsf{T}$, $a = 0, 1, \tau$ for $i = 1, 2, 3, 4$, $j = 1, 2, \ldots, N-1$. $q_{i,j}^\tau, p_{i,j}^\tau$ are polynomials in τ. The symbols "$\cdot 2$" and "$\cdot$" indicate the entrywise square operation and the entrywise multiplication operation, respectively.

It can be observed that p_i^τ can be eliminated from (40). If the generating quadrature formula has s nodes, then $A_{\tau,\sigma}$ is a polynomial of degree s in variable τ, so are $q_{i,j}^\tau$ for $i = 1, \ldots, 4$, $j = 0, 1, \ldots, N-1$. These polynomials are uniquely determined by their values at $s + 1$ points. For convenience, we choose $0, \frac{1}{s}, \frac{2}{s}, \ldots, 1$. Then $q_{i,j}^\tau$ can be expressed as Lagrange interpolating polynomials based on these $s + 1$ points. Fixing τ at $\frac{1}{s}, \frac{2}{s}, \ldots, \frac{s-1}{s}$, we get a system of algebraic equations in $q_{i,j}^c$, $c = 0, \frac{1}{s}, \frac{2}{s}, \ldots, 1$. The polynomial integrals in this system can be calculated accurately. Solving the algebraic system by an iteration method, we finally obtain the numerical solution $q_{i,j}^1$.

For example, if we select the CRK method generated by a 2-point GL quadrature formula, then q_i^σ, p_i^σ are vectors whose entries are polynomials of degree 2. Thus we have

$$q_i^\sigma = q_i^0 \tilde{l}_1(\sigma) + q_i^{\frac{1}{2}} \tilde{l}_2(\sigma) + q_i^1 \tilde{l}_3(\sigma),$$

where $\tilde{l}_1(\sigma), \tilde{l}_2(\sigma), \tilde{l}_3(\sigma)$ are Lagrange interpolating polynomials based on the nodes $0, \frac{1}{2}, 1$. Let $\tau = \frac{1}{2}$, the first four

equations of (40) can be written in practical forms :

$$q_1^{\frac{1}{2}} = q_1^0 + \Delta t \int_0^1 A_{\frac{1}{2},\sigma}(-\alpha D q_1^\sigma - D p_2^\sigma - (((q_1^\sigma)^{\cdot 2} + (q_2^\sigma)^{\cdot 2}) + \beta((q_3^\sigma)^{\cdot 2} + (q_4^\sigma)^{\cdot 2})) \cdot q_2^\sigma) d\sigma,$$

$$q_2^{\frac{1}{2}} = q_2^0 + \Delta t \int_0^1 A_{\frac{1}{2},\sigma}(-\alpha D q_2^\sigma + D p_1^\sigma + (((q_1^\sigma)^{\cdot 2} + (q_2^\sigma)^{\cdot 2}) + \beta((q_3^\sigma)^{\cdot 2} + (q_4^\sigma)^{\cdot 2})) \cdot q_1^\sigma) d\sigma,$$

$$q_3^{\frac{1}{2}} = q_3^0 + \Delta t \int_0^1 A_{\frac{1}{2},\sigma}(\alpha D q_3^\sigma - D p_4^\sigma - (\beta((q_1^\sigma)^{\cdot 2} + (q_2^\sigma)^{\cdot 2}) + ((q_3^\sigma)^{\cdot 2} + (q_4^\sigma)^{\cdot 2})) \cdot q_4^\sigma) d\sigma,$$

$$q_4^{\frac{1}{2}} = q_4^0 + \Delta t \int_0^1 A_{\frac{1}{2},\sigma}(\alpha D q_4^\sigma + D p_3^\sigma + (\beta((q_1^\sigma)^{\cdot 2} + (q_2^\sigma)^{\cdot 2}) + ((q_3^\sigma)^{\cdot 2} + (q_4^\sigma)^{\cdot 2})) \cdot q_3^\sigma) d\sigma. \tag{41}$$

After integrating the linear and nonlinear terms about σ, (41) becomes an undetermined system of equations in unknown vectors $q_1^{\frac{1}{2}}, q_2^{\frac{1}{2}}, q_3^{\frac{1}{2}}, q_4^{\frac{1}{2}}, q_1^1, q_2^1, q_3^1, q_4^1$. By combining them with the 5*th*, 6*th*, 7*th*, 8*th* equations of (40), we obtain an entirely determined algebraic system about them which can be easily solved by a fixed-point iteration in practical computations. If the generating quadrature formula has only one node, for example, the implicit midpoint rule, then $q_i^\sigma = (1 - \sigma)q_i^0 + \sigma q_i^1$. In this particular case, the first four equations are not necessary to be taken into account.

According to Theorem 3.1, the scheme (40) preserves the discrete ECLs:

$$\frac{E_j^1 - E_j^0}{\Delta t} + \sum_{k=0}^{N-1} D_{jk} \bar{F}_{jk} = 0, \tag{42}$$

for $j = 0, 1, \ldots, N - 1$, where

$$E_j^a = S_j^a - \alpha(q_{2,j}^a p_{1,j}^a - q_1^a p_{2,j}^a + q_{3,j}^a p_{4,j}^a - q_{4,j}^a p_{3,j}^a) - \frac{1}{2} \sum_{i=1}^4 (q_{i,j}^a \sum_{k=0}^{N-1} D_{jk} p_{i,k}^a - 2(p_{i,j}^a)^2), a = 0, 1,$$

$$\bar{F}_{jk} = \frac{1}{2} \sum_{i=1}^s b_i(\alpha(\langle q_{2,j}\rangle_i \langle \delta_t q_{1,k}\rangle_i - \langle q_{1,j}\rangle_i \langle \delta_t q_{2,k}\rangle_i + \langle q_{3,j}\rangle_i \langle \delta_t q_{4,k}\rangle_i - \langle q_{4,j}\rangle_i \langle \delta_t q_{3,k}\rangle_i) + \sum_{\gamma=1}^4 (\langle q_{\gamma,j}\rangle_i \langle \delta_t p_{\gamma,k}\rangle_i - \langle p_{\gamma,j}\rangle_i \langle \delta_t q_{\gamma,k}\rangle_i)$$

$$+ \alpha(\langle q_{2,k}\rangle_i \langle \delta_t q_{1,j}\rangle_i - \langle q_{1,k}\rangle_i \langle \delta_t q_{2,j}\rangle_i + \langle q_{3,k}\rangle_i \langle \delta_t q_{4,j}\rangle_i - \langle q_{4,k}\rangle_i \langle \delta_t q_{3,j}\rangle_i) + \sum_{\gamma=1}^4 (\langle q_{\gamma,k}\rangle_i \langle \delta_t p_{\gamma,j}\rangle_i - \langle p_{\gamma,k}\rangle_i \langle \delta_t q_{\gamma,j}\rangle_i)).$$

5. Local energy-preserving schemes for 2D nonlinear Schrödinger equations

Another PDE which we pay attention to is the NLS with two spatial variables:

$$i\psi_t + \alpha(\psi_{xx} + \psi_{yy}) + V'(|\psi|^2, x, y)\psi = 0. \tag{43}$$

The symbol $'$ indicates the derivative of V with respect to the first variable. Let $\psi = p + iq$, p and q are real and imaginary parts of ψ, respectively. Introducing $v = \partial_x p, w = \partial_x q, a = \partial_y p, b = \partial_y q$, we can formulate this equation to the compact form (20), where

$$M = \begin{pmatrix} 0 & 1 & 0 & 0 & 0 & 0 \\ -1 & 0 & 0 & 0 & 0 & 0 \\ 0 & 0 & 0 & 0 & 0 & 0 \\ 0 & 0 & 0 & 0 & 0 & 0 \\ 0 & 0 & 0 & 0 & 0 & 0 \\ 0 & 0 & 0 & 0 & 0 & 0 \end{pmatrix}, \quad K = \begin{pmatrix} 0 & 0 & -\alpha & 0 & 0 & 0 \\ 0 & 0 & 0 & -\alpha & 0 & 0 \\ \alpha & 0 & 0 & 0 & 0 & 0 \\ 0 & \alpha & 0 & 0 & 0 & 0 \\ 0 & 0 & 0 & 0 & 0 & 0 \\ 0 & 0 & 0 & 0 & 0 & 0 \end{pmatrix}, \quad L = \begin{pmatrix} 0 & 0 & 0 & 0 & -\alpha & 0 \\ 0 & 0 & 0 & 0 & 0 & -\alpha \\ 0 & 0 & 0 & 0 & 0 & 0 \\ 0 & 0 & 0 & 0 & 0 & 0 \\ \alpha & 0 & 0 & 0 & 0 & 0 \\ 0 & \alpha & 0 & 0 & 0 & 0 \end{pmatrix},$$

and

$$z = (p, q, v, w, a, b)^\mathsf{T}, \quad S = \frac{1}{2}V(p^2 + q^2, x, y) + \frac{\alpha}{2}(v^2 + w^2 + a^2 + b^2).$$

According to (21), the ECL of Equation (43) reads

$$\partial_t E + \partial_x F + \partial_y G = 0, \tag{44}$$

where

$$E = \frac{1}{2}V(p^2 + q^2, x, y) + \frac{\alpha}{2}(pv_x + qw_x + pa_y + qb_y),$$

$$F = \frac{\alpha}{2}(-pv_t - qw_t + vp_t + wq_t), \quad G = \frac{\alpha}{2}(-pa_t - qb_t + ap_t + bq_t).$$

(43) also has the local charge conservation law:

$$\partial_t C + \partial_x P + \partial_y Q = 0,$$

where

$$C = \frac{1}{2}(p^2 + q^2), P = \alpha(-vq + wp), Q = \alpha(-aq + bp).$$

If V is independent of the variables x, y, then (43) is a multi-symplectic PDE. According to (2), the MSCL is:

$$\partial_t(dp \wedge dq) + \partial_x(-\alpha dp \wedge dv - \alpha dq \wedge dw) + \partial_y(-\alpha dp \wedge da - \alpha dq \wedge db) = 0.$$

All of these conservation laws lead to corresponding global invariants under the PBC. The full discretized scheme of (43) in vector form derived from our discrete procedure (22) is:

$$
\begin{cases}
p^\tau = p^0 + \Delta t \int_0^1 A_{\tau,\sigma}(-(D_x \otimes I_M)\alpha w^\sigma - (I_N \otimes D_y)\alpha b^\sigma - V'((p^\sigma)^{\cdot 2} + (q^\sigma)^{\cdot 2}, x \otimes e_M, e_N \otimes y) \cdot q^\sigma)d\sigma, \\[2mm]
q^\tau = q^0 + \Delta t \int_0^1 A_{\tau,\sigma}((D_x \otimes I_M)\alpha v^\sigma + (I_N \otimes D_y)\alpha a^\sigma + V'((p^\sigma)^{\cdot 2} + (q^\sigma)^{\cdot 2}, x \otimes e_M, e_N \otimes y) \cdot p^\sigma)d\sigma, \\[2mm]
p^1 = p^0 + \Delta t \int_0^1 (-(D_x \otimes I_M)\alpha w^\sigma - (I_N \otimes D_y)\alpha b^\sigma - V'((p^\sigma)^{\cdot 2} + (q^\sigma)^{\cdot 2}, x \otimes e_M, e_N \otimes y) \cdot q^\sigma)d\sigma, \\[2mm]
q^1 = q^0 + \Delta t \int_0^1 (D_x \otimes I_M)\alpha v^\sigma + (I_N \otimes D_y)\alpha a^\sigma + V'((p^\sigma)^{\cdot 2} + (q^\sigma)^{\cdot 2}, x \otimes e_M, e_N \otimes y) \cdot p^\sigma)d\sigma, \\[2mm]
\delta_x p^\sigma = (D_x \otimes I_M)p^\sigma = v^\sigma, \delta_x q^\sigma = (D_x \otimes I_M)q^\sigma = w^\sigma, \\[2mm]
\delta_y p^\sigma = (I_N \otimes D_y)p^\sigma = a^\sigma, \delta_y q^\sigma = (I_N \otimes D_y)q^\sigma = b^\sigma,
\end{cases}
\tag{45}
$$

where the entries p_{jl}, q_{jl} of vectors p, q are arranged according to lexicographical order :

$$(j, l) \prec (k, l), \text{ when } j \prec k, \quad (j, l) \prec (j, m), \text{ when } l \prec m,$$

$x = (x_0, x_1, \ldots, x_{N-1})^\mathsf{T}, y = (y_0, y_1, \ldots, y_{M-1})^\mathsf{T}$, I_N, I_M, e_N, e_M are Nth and Mth order identity matrices, N length and M length identity vectors, respectively. If the potential V is a polynomial in the first variable, then the scheme (45) can be implemented in a similar way to (40).

By Theorem 3.2, (45) preserves the discrete ECLs:

$$\frac{E_{jl}^1 - E_{jl}^0}{\Delta t} + \sum_{k=0}^{N-1}(D_x)_{jk}\bar{F}_{jk,l} + \sum_{m=0}^{M-1}(D_y)_{lm}\bar{G}_{j,lm} = 0, \tag{46}$$

for $j = 0, 1, \ldots, N - 1, l = 0, 1, \ldots, M - 1$, where

$$E_{jl}^c = \frac{1}{2}V((p_{jl}^c)^2 + (q_{jl}^c)^2, x_j, y_l) + \frac{\alpha}{2}(p_{jl}^c\delta_x v_{jl}^c + q_{jl}^c\delta_x w_{jl}^c + p_{jl}^c\delta_y a_{jl}^c + q_{jl}^c\delta_y b_{jl}^c), c = 0, 1,$$

$$\bar{F}_{jk,l} = \frac{\alpha}{2}\sum_{i=1}^{s} b_i(-\langle p_{jl}\rangle_i\langle\delta_t v_{kl}\rangle_i - \langle q_{jl}\rangle_i\langle\delta_t w_{kl}\rangle_i + \langle v_{jl}\rangle_i\langle\delta_t p_{kl}\rangle_i + \langle w_{jl}\rangle_i\langle\delta_t q_{kl}\rangle_i$$

$$+ \frac{\alpha}{2}\sum_{i=1}^{s} b_i(-\langle p_{kl}\rangle_i\langle\delta_t v_{jl}\rangle_i - \langle q_{kl}\rangle_i\langle\delta_t w_{jl}\rangle_i + \langle v_{kl}\rangle_i\langle\delta_t p_{jl}\rangle_i + \langle w_{kl}\rangle_i\langle\delta_t q_{jl}\rangle_i),$$

$$\bar{G}_{j,lm} = \frac{\alpha}{2}\sum_{i=1}^{s} b_i(-\langle p_{jl}\rangle_i\langle\delta_t a_{jm}\rangle_i - \langle q_{jl}\rangle_i\langle\delta_t b_{jm}\rangle_i + \langle a_{jl}\rangle_i\langle\delta_t p_{jm}\rangle_i + \langle b_{jl}\rangle_i\langle\delta_t q_{jm}\rangle_i)$$

$$+ \frac{\alpha}{2}\sum_{i=1}^{s} b_i(-\langle p_{jm}\rangle_i\langle\delta_t a_{jl}\rangle_i - \langle q_{jm}\rangle_i\langle\delta_t b_{jl}\rangle_i + \langle a_{jm}\rangle_i\langle\delta_t p_{jl}\rangle_i + \langle b_{jm}\rangle_i\langle\delta_t q_{jl}\rangle_i).$$

However, the expressions of E_{jl}^c, $\bar{F}_{jk,l}$, $\bar{G}_{j,lm}$ are lengthy and difficult to be calculated. We thus rewrite them as:

$$
\begin{aligned}
E_{jl}^c &= \frac{1}{2}V((p_{jl}^c)^2 + (q_{jl}^c)^2, x_j, y_l) - \frac{\alpha}{2}((v_{jl}^c)^2 + (w_{jl}^c)^2 + (a_{jl}^c)^2 + (b_{jl}^c)^2) + \tilde{E}_{jl}^c, c = 0, 1, \\
\bar{F}_{jk,l} &= \alpha \sum_{i=1}^{s} b_i(\langle v_{jl}\rangle_i \langle \delta_t p_{kl}\rangle_i + \langle w_{jl}\rangle_i \langle \delta_t q_{kl}\rangle_i + \langle v_{kl}\rangle_i \langle \delta_t p_{jl}\rangle_i + \langle w_{kl}\rangle_i \langle \delta_t q_{jl}\rangle_i) + \tilde{F}_{jk,l}, \\
\bar{G}_{j,lm} &= \alpha \sum_{i=1}^{s} b_i(\langle a_{jl}\rangle_i \langle \delta_t p_{jm}\rangle_i + \langle b_{jl}\rangle_i \langle \delta_t q_{jm}\rangle_i + \langle a_{jm}\rangle_i \langle \delta_t p_{jl}\rangle_i + \langle b_{jm}\rangle_i \langle \delta_t q_{jl}\rangle_i) + \tilde{G}_{j,lm},
\end{aligned}
\tag{47}
$$

where $\tilde{E}_{jl}^c$, $\tilde{F}_{jk,l}$ $\tilde{G}_{j,lm}$ are the corresponding residuals. Taking derivatives with respect to τ on both sides of

$$
\delta_x p_{jl}^\tau = v_{jl}^\tau = v_{jl}^0 + \Delta t \int_0^1 A_{\tau,\sigma} \delta_t v_{jl}^\sigma d\sigma
$$

and setting $\tau = c_1, \ldots, c_s$, we have

$$
\langle \delta_x \delta_t p_{jl}\rangle_i = \langle \delta_t v_{jl}\rangle_i,
$$

for $i = 1, \ldots, s$. By using this law of commutation and following the standard proof procedure of Theorem 3.1, the term involving v_{jl} can be eliminated from $\tilde{E}_{jl}^c$, $\tilde{F}_{jk,l}$ $\tilde{G}_{j,lm}$. The terms involving w_{jl}, a_{jl}, b_{jl} can be dealt with in the same way.

Therefore we arrive at

$$
\frac{\tilde{E}_{jl}^1 - \tilde{E}_{jl}^0}{\Delta t} + \sum_{k=0}^{N-1}(D_x)_{jk}\tilde{F}_{jk,l} + \sum_{m=0}^{M-1}(D_y)_{lm}\tilde{G}_{j,lm} = 0.
\tag{48}
$$

Subtracting (48) from (46), we obtain the new discree ECLs of (45)

$$
\frac{E_{jl}^1 - E_{jl}^0}{\Delta t} + \sum_{k=0}^{N-1}(D_x)_{jk}\bar{F}_{jk,l} + \sum_{m=0}^{M-1}(D_y)_{lm}\bar{G}_{j,lm} = 0,
\tag{49}
$$

for $j = 0, 1, \ldots, N - 1$, $\quad l = 0, 1, \ldots, M - 1$, where

$$
\begin{aligned}
E_{jl} &= \frac{1}{2}V(p_{jl}^2 + q_{jl}^2, x_j, y_l) - \frac{\alpha}{2}(v_{jl}^2 + w_{jl}^2 + a_{jl}^2 + b_{jl}^2), \\
\bar{F}_{jk,l} &= \alpha \sum_{i=1}^{s} b_i(\langle v_{jl}\rangle_i \langle \delta_t p_{kl}\rangle_i + \langle w_{jl}\rangle_i \langle \delta_t q_{kl}\rangle_i + \langle v_{kl}\rangle_i \langle \delta_t p_{jl}\rangle_i + \langle w_{kl}\rangle_i \langle \delta_t q_{jl}\rangle_i), \\
\bar{G}_{j,lm} &= \alpha \sum_{i=1}^{s} b_i(\langle a_{jl}\rangle_i \langle \delta_t p_{jm}\rangle_i + \langle b_{jl}\rangle_i \langle \delta_t q_{jm}\rangle_i + \langle a_{jm}\rangle_i \langle \delta_t p_{jl}\rangle_i + \langle b_{jm}\rangle_i \langle \delta_t q_{jl}\rangle_i).
\end{aligned}
$$

(49) can be thought of as a discrete version of

$$
\partial_t(\frac{1}{2}V(p^2 + q^2, x, y)) + \partial_x(vp_t + wq_t) + \partial_y(ap_t + bq_t) = 0,
$$

which is a more common ECL equation (43) than (44).

(49) involve less discrete derivatives than (46), thus can be easily calculated.

6. Numerical experiments for coupled nonlinear Schrödingers equations

If we choose the two-point Gauss-Legendre quadrature formula:

$$
b_1 = \frac{1}{2}, b_2 = \frac{1}{2},
$$

$$
c_1 = \frac{1}{2} - \frac{\sqrt{3}}{6}, c_2 = \frac{1}{2} + \frac{\sqrt{3}}{6}
$$

for the CRK method, then

$$A_{\tau,\sigma} = \tau((4 - 3\tau) - 6(1 - \tau)\sigma).$$

This CRK method is of order four by (6). In this section, we use it for the temporal discretization while the spatial direction is discretized by the pseudospectral method. The corresponding local energy-preserving method for the CNLS is denoted by ET4.

Throughout the experiments in this section we always take the periodic boundary condition $u(x_0, t) = u(x_0 + L, t)$, $v(x_0, t) = v(x_0 + L, t)$ and set the initial time $t_0 = 0$. Besides the discrete global energy which has been mentioned in (14), we define these discrete global quantities as follows:

1. The discrete global charges of u and v at time $n\Delta t$:

$$
\begin{cases}
CH_U^n = \Delta x \sum_{j=0}^{N-1} ((q_{1,j}^n)^2 + (q_{2,j}^n)^2), \\
CH_V^n = \Delta x \sum_{j=0}^{N-1} ((q_{3,j}^n)^2 + (q_{4,j}^n)^2).
\end{cases}
$$

2. The discrete global momentum at time $n\Delta t$:

$$I^n = \Delta x \sum_{j=0}^{N-1} (q_{2,j}^n p_{1,j}^n - q_{1,j}^n p_{2,j}^n + q_{4,j}^n p_{3,j}^n - q_{3,j}^n p_{4,j}^n).$$

The (relative) global energy error (GEE^n), global momentum error (GIE^n), global charge errors of u (GCE$_U^n$) and v (GCE$_V^n$) at time $n\Delta t$ will be calculated by the following formulas :

$$
GGE^n = \frac{E^n - E^0}{|E^0|}, GIE^n = \frac{I^n - I^0}{|I^0|},
$$

$$
GCE_U^n = \frac{CH_U^n - CH_U^0}{|CH_U^0|}, GCE_V^n = \frac{CH_V^n - CH_V^0}{|CH_V^0|},
$$

respectively.

Experiment 6.1. *We first consider to set the constants $\alpha, \beta = 0$. Then the CNLS decompose into two independent NLSs:*

$$
\begin{cases}
iu_t + \dfrac{1}{2}u_{xx} + |u|^2 u = 0, \\
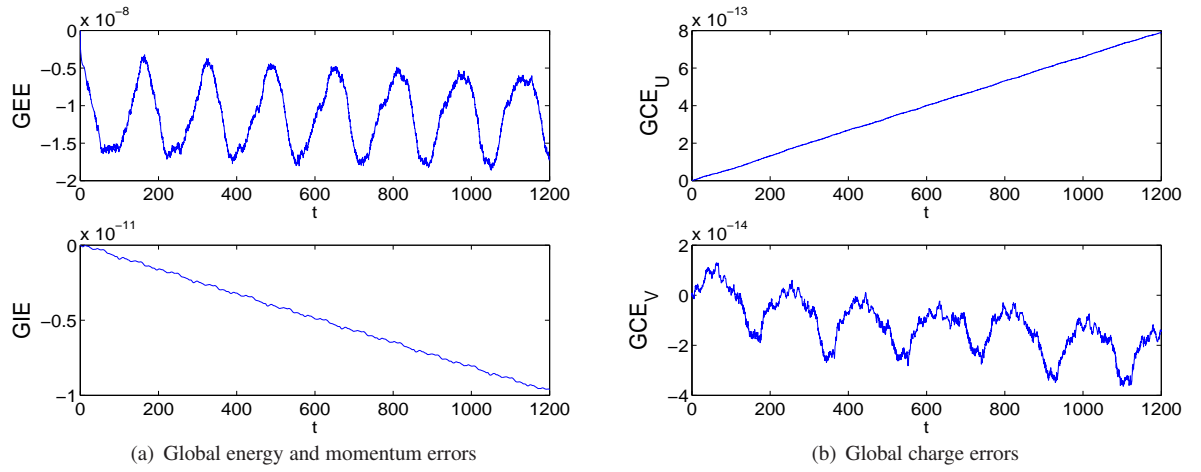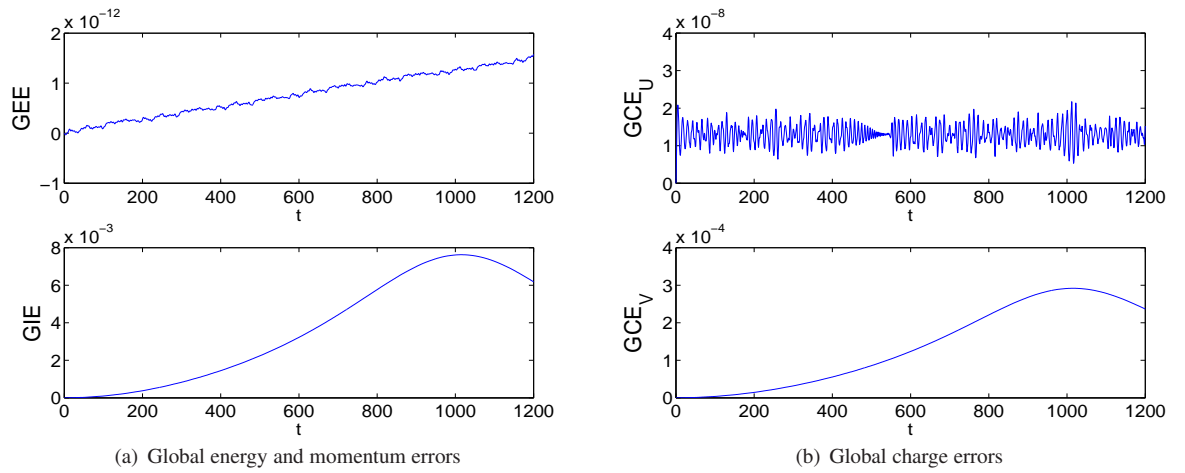iv_t + \dfrac{1}{2}v_{xx} + |v|^2 v = 0.
\end{cases}
\tag{50}
$$

Given the initial condition:

$$
\begin{cases}
u(x, 0) = sech(x), \\
v(x, 0) = sech(x)exp(i\dfrac{x}{\sqrt{10}}),
\end{cases}
$$

the analytic expressions of u and v are :

$$
\begin{cases}
u(x, t) = sech(x)exp(i\dfrac{t}{2}), \\
v(x, t) = sech(x - \dfrac{t}{\sqrt{10}})exp(i(\dfrac{x}{\sqrt{10}} + \dfrac{9}{20}t)).
\end{cases}
\tag{51}
$$

In this experiment, we compute the difference between the numerical solution and the exact solution of u. Since u decays exponentially away from the point $(0, t)$, we can take the boundary condition $u(-30, 0) = u(30, 0)$, $v(-30, 0) = v(30, 0)$ with little loss of accuracy on u. We also compare our local energy-preserving method ET4 with a classical multi-symplectic scheme (MST4) which is obtained by concatenating the two-point Gauss-Legendre symplectic Runge–Kutta method in time and the pseudospectral method in space. Note that ET4 and MST4 are of the same order. Let $N = 300$, $\Delta t = 0.4$, 0.8 and set $\varepsilon = 10^{-14}$ as the error tolerance for iteration solutions. The numerical results over the time interval $[0, 1200]$, which is about 100 multiples of the period of u, are plotted in Figs. 1,...,6.

(a) Global energy and momentum errors

(b) Global charge errors
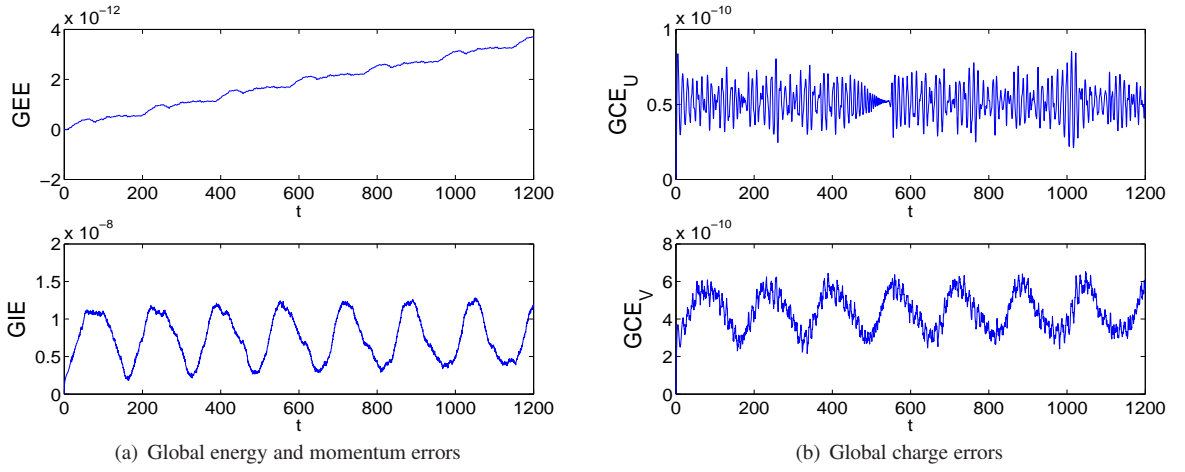
Figure 1: Errors obtained by ET4, $\Delta t = 0.4$.

(a) Global energy and momentum errors

(b) Global charge errors

Figure 2: Errors obtained by MST4, $\Delta t = 0.4$.

(a) Global energy and momentum errors

(b) Global charge errors

Figure 3: Errors obtained by ET4, $\Delta t = 0.8$.

(a) Global energy and momentum errors   (b) Global charge errors
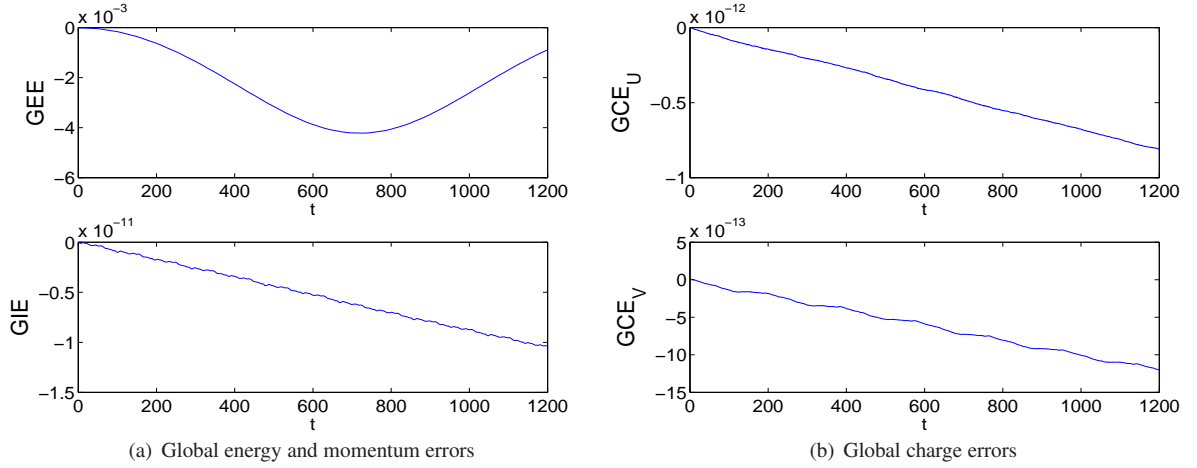
Figure 4: Errors obtained by MST4, Δt=0.8.

(a) Maximum global errors, $\Delta t = 0.4$.   (b) Maximum global errors, $\Delta t = 0.8$.
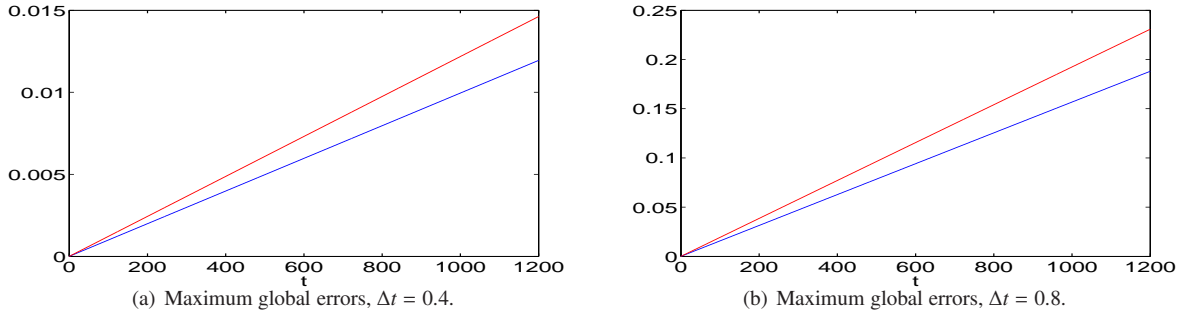
Figure 5: Maximum global errors of ET4 (left) and MST4 (right) . The blue and red curves are the errors of ET4 and MST4 respectively.

Figs. 1, 3 illustrate that ET4 conserves the discrete global energy exactly (regardless of round-off errors). Although ET4 cannot preserve discrete global charges, its global charge errors show reasonable oscillation in magnitude 10^{-10} ($\Delta t = 0.4$) and 10^{-4} ($\Delta t = 0.8$), respectively. We attribute this behaviour to the conjugate-symplecticity of the CRK method.

On the contrary, Figs. 2, 4 show that MST4 conserves global charges exactly (regardless of round-off errors) while its global energy errors oscillates in magnitude 10^{-8} ($\Delta t = 0.4$) and 10^{-3} ($\Delta t = 0.8$). This is a character of symplectic integrators.

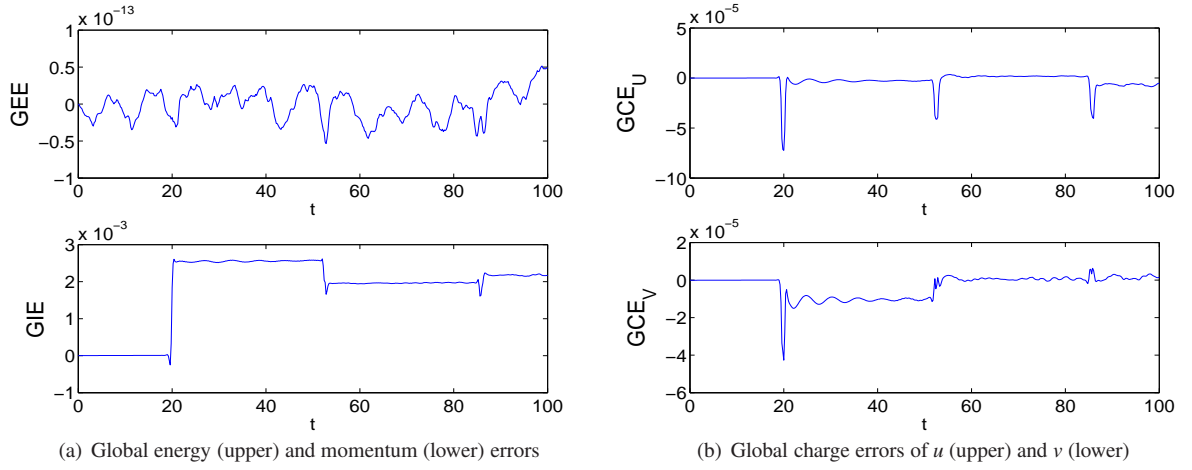*According to Figs. 1,…,4, MST4 preserves the discrete global momentum better than ET4 in this experiment.*

It can be observed from (51) that the amplitudes of u and v are both 1. Fig. 5 shows that ET4 and MST4 both have excellent long-term behaviours. The relative maximum global errors do not exceed 1.5% ($\Delta t = 0.4$) and 25% ($\Delta t = 0.8$) over the time interval [0,1200] .

Here we point out that ET4 and ST4 have the same iteration cost with the same Δt and ε. In the case $\Delta t = 0.4$, both of them need 19 iterations per step. This phenomenon also occurs in the following experiments.

Experiment 6.2. *We now start to simulate the collision of double solitons with the initial condition:*

$$\begin{cases} u(x,0) = \displaystyle\sum_{j=1}^{2} \sqrt{\frac{2a_j}{1+\beta}} sech(\sqrt{2a_j}(x-x_j))exp(i(\gamma_j - \alpha)(x - x_j)), \\[2mm] v(x,0) = \displaystyle\sum_{j=1}^{2} \sqrt{\frac{2a_j}{1+\beta}} sech(\sqrt{2a_j}(x-x_j))exp(i(\gamma_j + \alpha)(x - x_j)). \end{cases}$$

This is an initial condition resulting in a collision of two separate single solitons. Here we choose $x_0 = 0, L = 100, \alpha =$
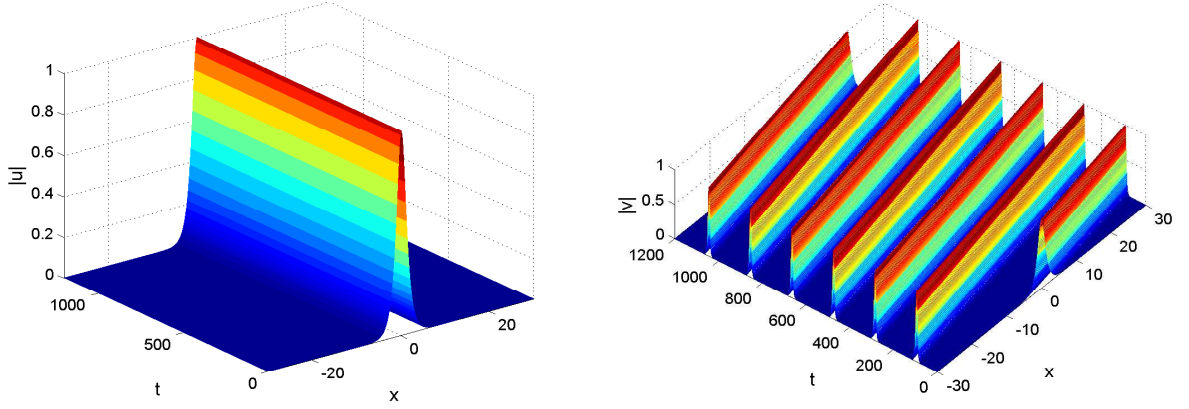
Figure 6: Numerical shapes of *u* (left) and *v* (right), obtained by ET4.

(a) Global energy (upper) and momentum (lower) errors

(b) Global charge errors of *u* (upper) and *v* (lower)

Figure 7: Errors obtained by ET4, $\Delta t = 0.2$, $N = 450$.

$0.5, \beta = \frac{2}{3}, a_1 = 1, a_2 = 0.8, \gamma_1 = 1.5, \gamma_2 = -1.5, x_1 = 20, x_2 = 80$. *Take the temporal stepsize $\Delta t = 0.2$ and spatial grid number $N = 450$. The numerical results are shown in Figs. 7, 8.*

Obviously, ET4 successfully simulates the collision of two solitons and the effects of boundaries on bisolitons. It preserves exactly the discrete energy and conserves the discrete charges and momentum very well.

Experiment 6.3. *The last experiment on the CNLS is the simulation of the interaction among triple solitons with the initial condition:*

$$\begin{cases} u(x,0) = \sum_{j=1}^{3} \sqrt{\frac{2a_j}{1+\beta}} sech(\sqrt{2a_j}(x - x_j))exp(i(\gamma_j - \alpha)(x - x_j), \\ v(x,0) = \sum_{j=1}^{3} \sqrt{\frac{2a_j}{1+\beta}} sech(\sqrt{2a_j}(x - x_j))exp(i(\gamma_j + \alpha)(x - x_j)). \end{cases}$$

Here we also test another scheme associated with ET4. The only difference between it and ET4 is that we evaluate the nonlinear integrals in ET4 not by symbol calculation, but by the high-order GL quadrature formula. In the case of ET4, the polynomials are of degrees 6, so we can calculate them exactly by a 4-point GL formula. To illustrate the

(a) The shape of bisoliton u

(b) The shape of bisoliton v
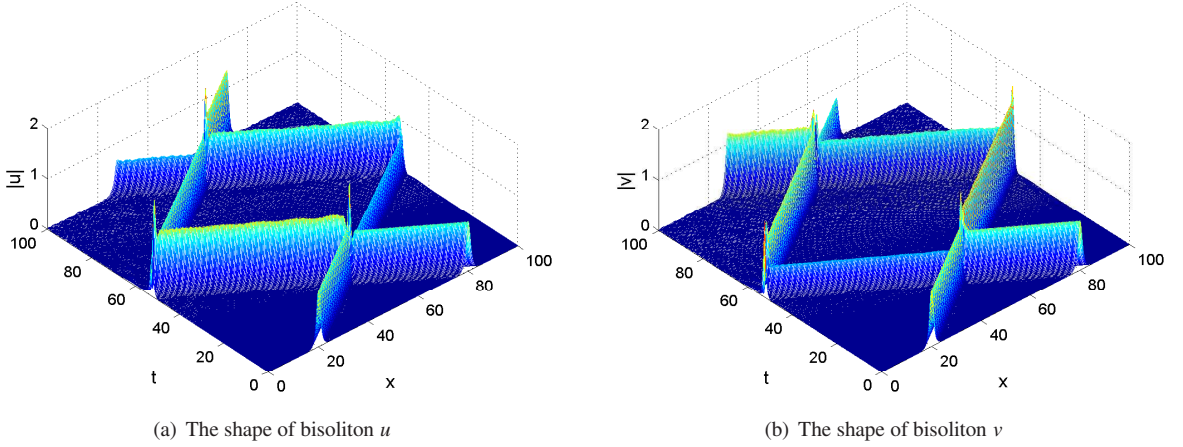
Figure 8: Numerical shapes of u (left) and v (right), obtained from ET4.

alternative scheme, we evaluate the nonlinear integrals by a 3-point GL formula:

$$b_1 = \frac{5}{18}, b_2 = \frac{4}{9}, b_3 = \frac{5}{18},$$

$$c_1 = \frac{1}{2} - \frac{\sqrt{15}}{10}, c_2 = \frac{1}{2}, c_3 = \frac{1}{2} + \frac{\sqrt{15}}{10}.$$

For example, the first nonlinear integral of (40) *is approximated by*

$$\int_0^1 (((q_1^\sigma)^{\cdot 2} + (q_2^\sigma)^{\cdot 2}) + \beta((q_3^\sigma)^{\cdot 2} + (q_4^\sigma)^{\cdot 2})) \cdot q_2^\sigma d\sigma$$

$$\approx \sum_{i=1}^{3} b_i(((q_1^{c_i})^{\cdot 2} + (q_2^{c_i})^{\cdot 2}) + \beta((q_3^{c_i})^{\cdot 2} + (q_4^{c_i})^{\cdot 2})) \cdot q_2^{c_i}.$$

For convenience, we denote the scheme by ET4GL6. Setting $\Delta t = 0.2, N = 360, x_0 = 0, L = 80, \alpha = 0.5, \beta = \frac{2}{3}, \gamma_1 = 1.5, \gamma_2 = 0.1, \gamma_3 = -1.2, a_1 = 0.75, a_2 = 1, a_3 = 0.5, x_1 = 20, x_2 = 40, x_3 = 60$, we compute it over the time interval [0,100]. Numerical results are presented in Figs. 9, ..., 12. The behaviours of ET4, ET4GL6 are very similar in conserving momentum. Unsurprisingly, ET4 and ST4 preserve exactly the discrete global energy and charges, respectively. However, ET4GL6 can conserve the discrete energy in magnitude 10^{-6}, while ST4 only preserves the energy in magnitude 10^{-4}. So if we give more weight on the discrete energy, ET4GL6 is a favourable scheme. In fact, when the nonlinear integrals cannot be calculated exactly or have to be integrated in very complicated forms, ETGL6 is a reasonable alternative scheme.
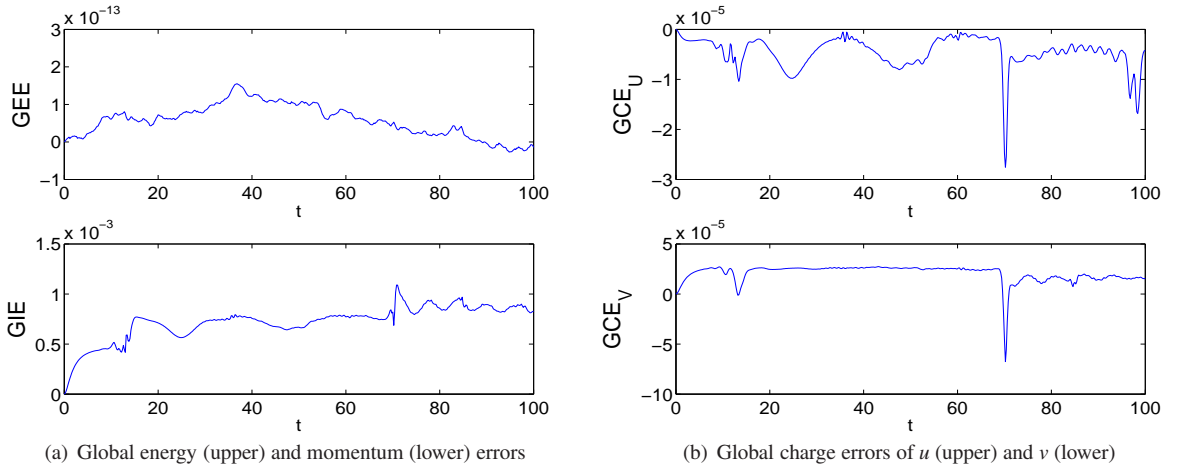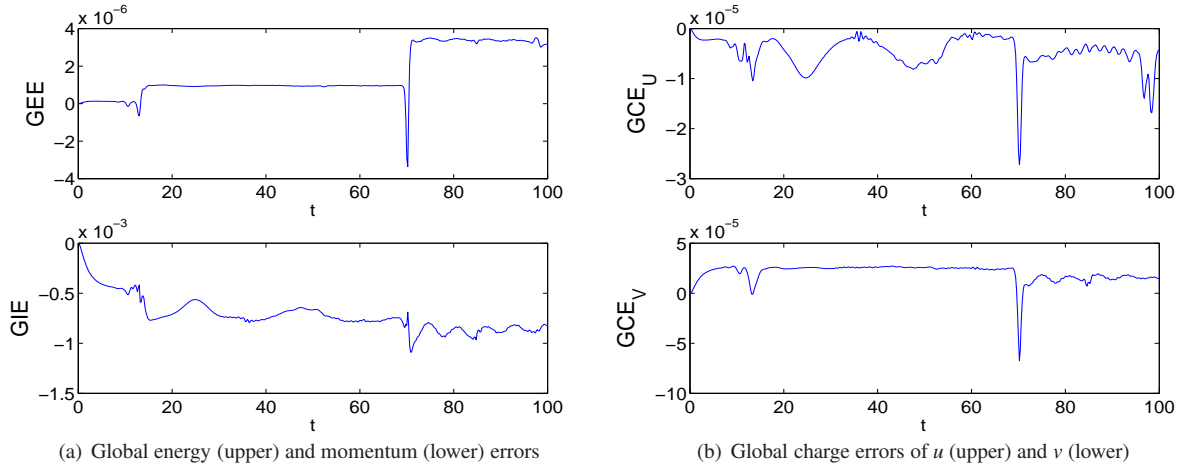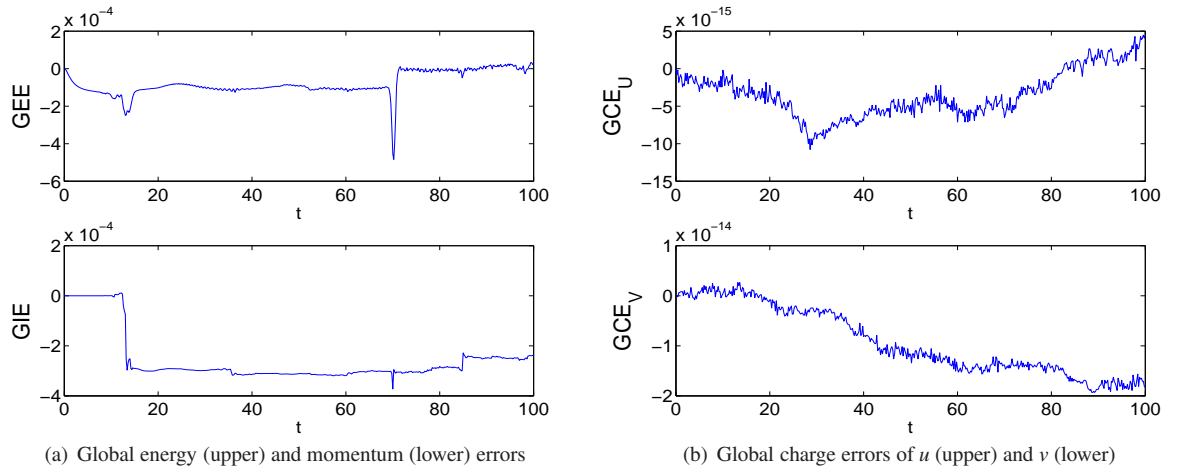
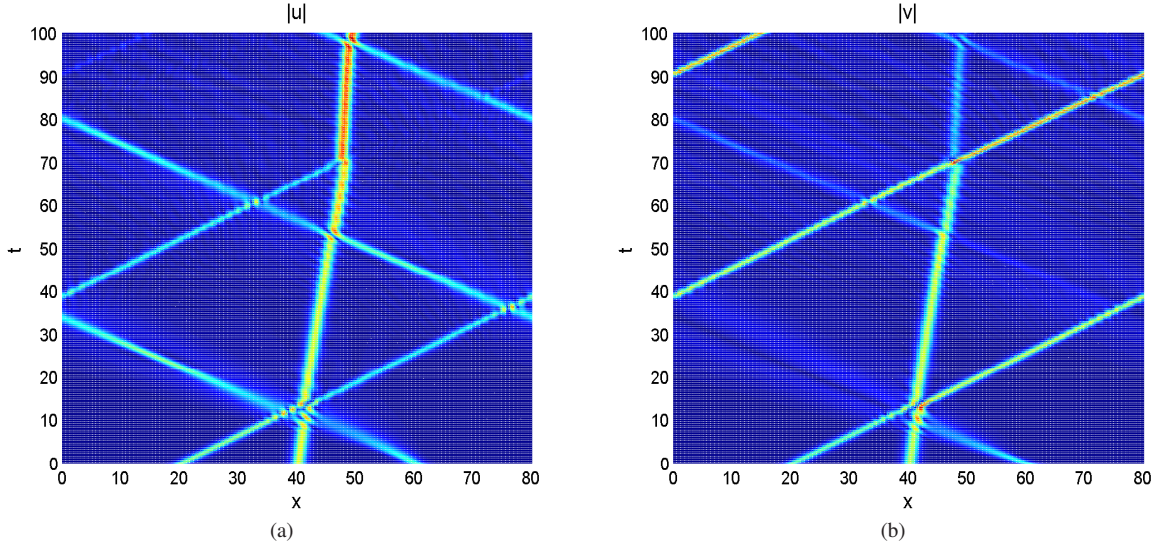## 7. Numerical experiments for 2D nonlinear Schrödinger equations

In this section, we apply the CRK method of second-order (i.e. average vector field method) to t-direction and the pseudospectral method to x and y directions. This scheme is denoted by ET2. To illustrate our method, we will compare it with another prominent traditional scheme which is obtained by the implicit midpoint temporal discretization and the pseudospectral spatial discretization(ST2). If (43) is linear, our scheme ET2 is the same as ST2. Hence we will not give numerical examples of 2D linear Schrödinger equations.

The boundary condition is always taken to be periodic:

$$u(x_l, y, t) = u(x_r, y, t), u(x, y_l, t) = u(x, y_r, t). \tag{52}$$

And the grid numbers of x and y directions are denoted by N and M, respectively.

(a) Global energy (upper) and momentum (lower) errors

(b) Global charge errors of *u* (upper) and *v* (lower)

Figure 9: Errors obtained by ET4, $\Delta t = 0.2$, $N = 360$.

(a) Global energy (upper) and momentum (lower) errors

(b) Global charge errors of *u* (upper) and *v* (lower)

Figure 10: Errors obtained by ET4GL6, $\Delta t = 0.2$, $N = 360$.

(a) Global energy (upper) and momentum (lower) errors

(b) Global charge errors of *u* (upper) and *v* (lower)

Figure 11: Errors obtained by ST4, $\Delta t = 0.2$, $N = 360$.

Figure 12: Numerical solitons of u, v, obtained by ET4.

The discrete global charge CH will still be taken into account:

$$CH^n = \Delta x \Delta y \sum_{j=0}^{N-1} \sum_{l=0}^{M-1} ((p_{jl}^n)^2 + (q_{jl}^n)^2),$$

where

$$CH^n \approx \int_{x_l}^{x_r} \int_{y_l}^{y_r} (p(x, y, n\Delta t)^2 + q(x, y, n\Delta t)^2) dx dy.$$

Besides, the residuals in the ECL (49) are defined as:

$$R_{jl}^n = \frac{E_{jl}^{n+1} - E_{jl}^n}{\Delta t} + \sum_{k=0}^{N-1} (D_x)_{jk} \bar{F}_{jk,l} + \sum_{m=0}^{M-1} (D_y)_{lm} \bar{G}_{j,lm},$$

for $j = 0, 1, \ldots, N-1, \quad l = 0, 1, \ldots, M-1$.

In this section, we calculate $\mathbf{R}^n$: the residual with the maximum absolute value at the time level $n\Delta t$.

Experiment 7.1. *Let $\alpha = \frac{1}{2}, V(\xi, x, y) = V_1(x, y)\xi + \frac{1}{2}\beta\xi^2$, then (43) becomes the Gross–Pitaevskii (GP) equation:*

$$i\psi_t + \frac{1}{2}(\psi_{xx} + \psi_{yy}) + V_1(x, y)\psi + \beta|\psi|^2\psi = 0. \tag{53}$$

This equation is an important mean-field model for the dynamics of a dilute gas Bose-Einstein condensate (BEC) (see, e.g. [12]). The parameter β determines whether (53) is attractive ($\beta > 0$) or repulsive ($\beta < 0$).

Note that equation (53) is no longer multi-symplectic, the scheme ST2 is only symplectic in time. We first consider the attractive case $\beta = 1$. The external potential V_1 is:

$$V_1(x, y) = -\frac{1}{2}(x^2 + y^2) - 2exp(-(x^2 + y^2)).$$

The initial condition is given by:

$$\psi(x, y, 0) = \sqrt{2}exp(-\frac{1}{2}(x^2 + y^2)).$$

This IVP has the exact solution (see, e.g. [1]):

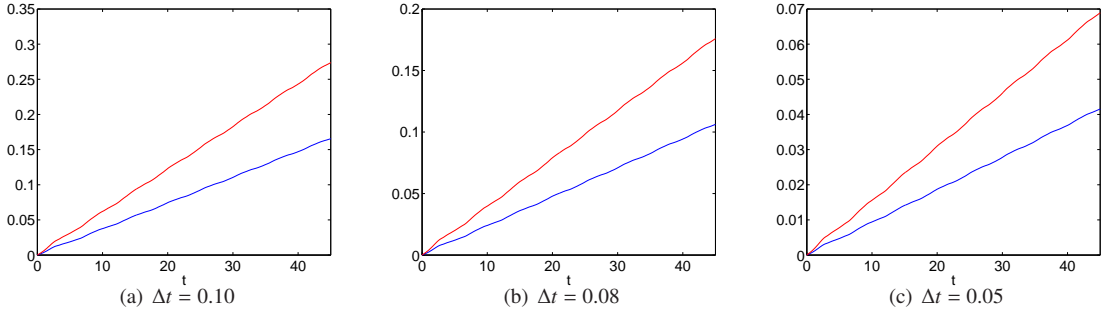$$\psi(x, y, t) = \sqrt{2}exp(-\frac{1}{2}(x^2 + y^2))exp(-it).$$

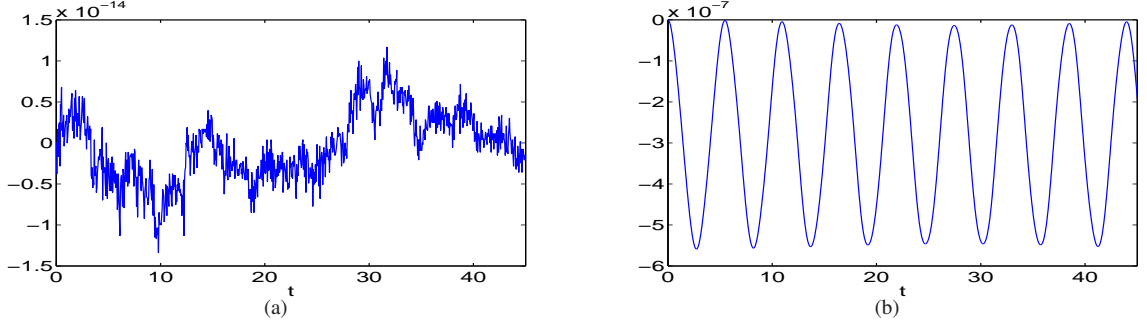Figure 13: Maximum global errors. The blue curves are the results of ET2, the red curves are the results of ST2.

Figure 14: Global energy errors of ET2 (left) and ST2 (right), $\Delta t = 0.05$.

For the same reason in the experiment 6.1, we set the spatial domain as $x_l = -6, x_r = 6, y_l = -6, y_r = 6$. The temporal stepzie is chosen as $\Delta t = 0.15, 0.1, 0.05$, respectively. Fixing the number of spatial grids $N = M = 42$, we compute the numerical solution over the time interval $[0, 45]$. The numerical results of ET2 and ST2 are shown in Figs. 13, ..., 16.

From the results, we can see that ET2 conserves both the global energy and the ECL exactly while its global charge errors oscillates in magnitude 10^{-7}. On the other hand, ST2 preserves the global charge accurately while its global energy errors oscillates in magnitude 10^{-7} and its maximum residuals in the ECL oscillates in magnitude 10^{-6}. However, the maximum global errors of ST2 are twice as large as that of ET2 under the three different Δt.

Experiment 7.2. *Let $V_1(x, y) = -\frac{1}{2}(x^2 + y^2), \beta = -2$. Given the initial condition*

$$\psi(x, y, 0) = \frac{1}{\sqrt{\pi}} exp(-\frac{1}{2}(x^2 + y^2)),$$

we now consider the repulsive GP equation in space $[-8, 8] \times [-8, 8]$ (see [22]). Let $N = M = 36, \Delta t = 0.1$, we
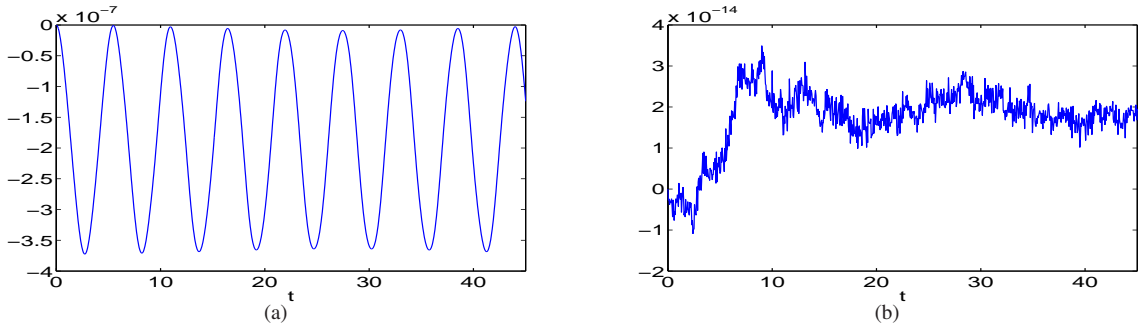

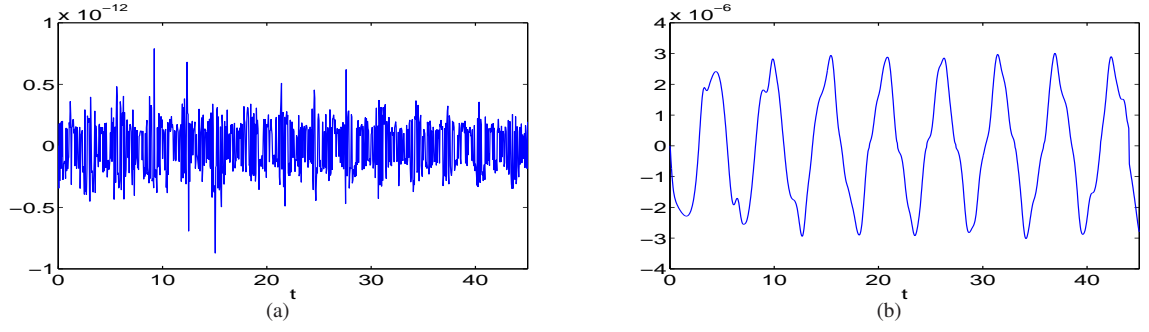Figure 15: Global charge errors of ET2 (left) and ST2 (right), $\Delta t = 0.05$.

Figure 16: Maximum residuals (**R**) of ET2 (left) and ST2 (right) in the ECL, $\Delta t = 0.05$.

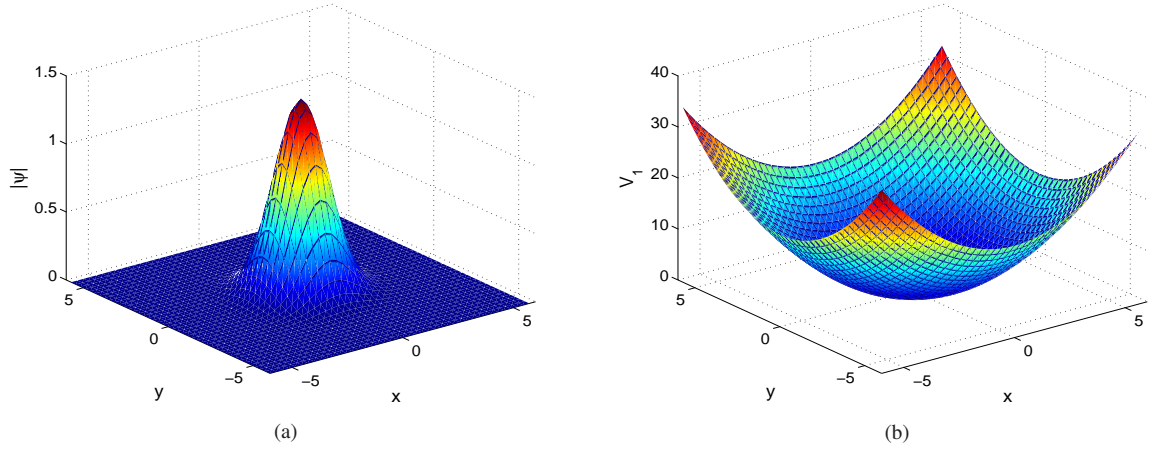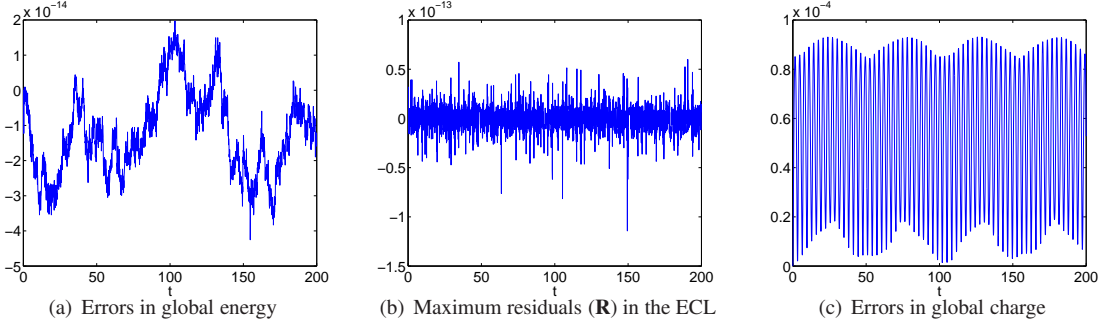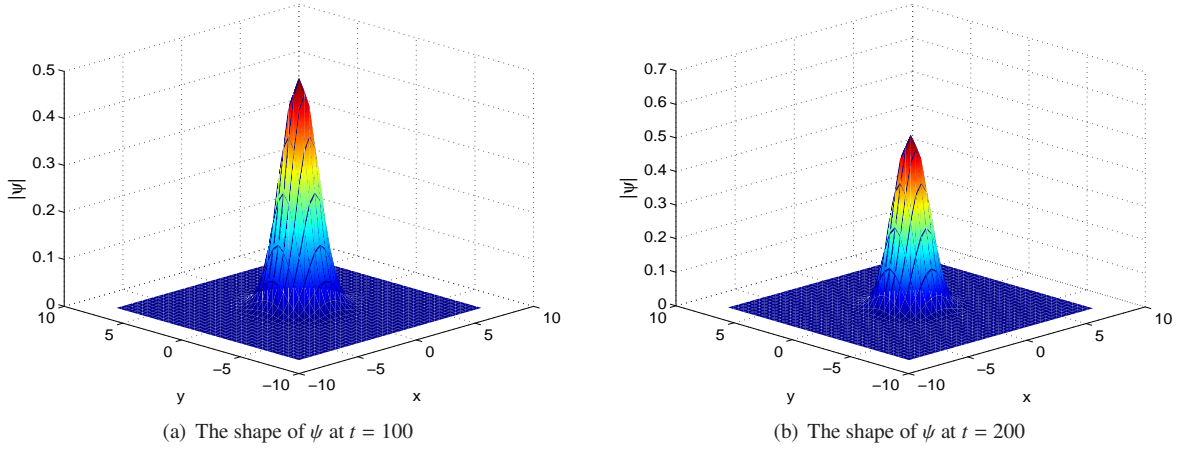Figure 17: Shapes of the solution (left) and the potential V_1 (right).

(a) Errors in global energy   (b) Maximum residuals (**R**) in the ECL   (c) Errors in global charge

Figure 18: Errors obtained by ET2.

(a) The shape of ψ at $t = 100$ (b) The shape of ψ at $t = 200$

Figure 19: The numerical shapes of ψ.

compute the numerical solution over the time interval $[0, 200]$. *The results are plotted in Figs. 18, 19. Obviously, ET2 still show the eminent long-term behaviour dealing with high dimensional problems.*

Experiment 7.3. *We then consider the 2DNLS with quintic nonlinearity:*

$$i\psi_t + \psi_{xx} + \psi_{yy} + V_1(x, y)\psi + |\psi|^4\psi = 0, \tag{54}$$

where

$$V_1(x, y) = -A^4(4A^4(x^2 + y^2) - exp(-A^4(x^2 + y^2)))$$

is an external field, and A is a constant. Its potential is:

$$V(\xi, x, y) = V_1(x, y)\xi + \frac{1}{3}\xi^3.$$

This equation admits the solution:

$$\psi(x, y, t) = Aexp(-\frac{1}{4}A^4(x^2 + y^2))exp(-iA^4t).$$

Its period is $\frac{2\pi}{A^4}$. *Set* $A = 1.5, x_l = -4, x_r = 4, y_l = -4, y_r = 4, \Delta t = 0.01, N = M = 42$. *We integrate (54) over a very long interval [0,124] which is about 100 multiples of the period. Since the behaviours of ET2 and ST2 in conserving the global charge and the energy are very similar to those in Experiments 7.1 and 7.2, they are omitted here. The global errors of ET2 and ST2 in l^∞ and $\frac{1}{\sqrt{NM}}l^2$ norms are shown in Fig. 20.*

Clearly, in the quintic case, our method again wins over the classical symplectic scheme ST2.
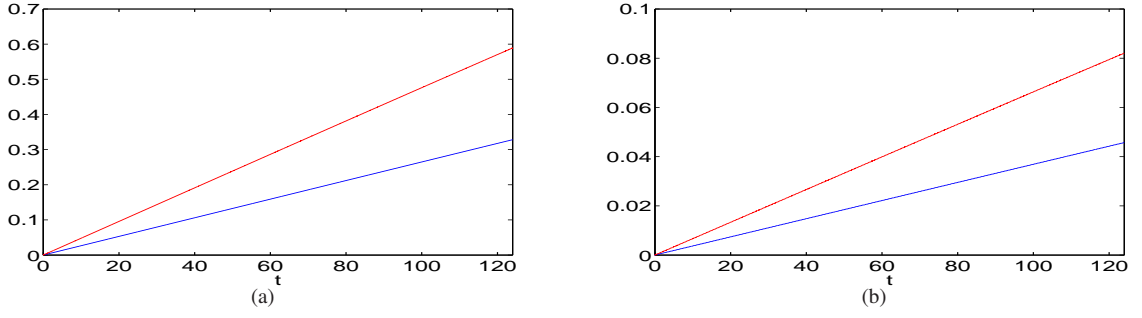
Figure 20: l^∞ global errors (left) and $\frac{1}{\sqrt{NM}} l^2$ global errors (right). The blue and red curves are obtained by ET2 and ST2 respectively.

8. Conclusions

"For Hamiltonian differential equations there is a long-standing dispute on the question whether in a numerical simulation it is more important to preserve energy or symplecticity. Many people give more weight on symplecticity, because it is known (by backward error analysis arguments) that symplectic integrators conserve a modified Hamiltonian" (Quote from Hairer's paper [17]).

However, due to the complexity of PDEs, the theory on multi-symplectic integrators is still far from being satisfactory. There are only a few results on some simple box schemes (e.g. the Preissman and the Euler box scheme) and on special PDEs (e.g. the nonlinear wave equation and the nonlinear Schrödinger equation) based on backward error analysis (see, e.g. [5, 20, 28]). These theories show that a class of box schemes conserves the modified ECL and MCL(see, e.g. [20]). Besides, it seems there is no robust theoretical results for the multi-symplectic (pseudo) spectral scheme. Therefore, the local energy-preserving algorithms may play a much more important role in PDEs than their counterparts in ODEs.

In this paper, we presented a general local energy-preserving method which can have arbitrarily high order for solving multi-symplectic Hamiltonian PDEs. In our method, time is discretized by a continuous Runge–Kutta method and space is discretized by a pseudospectral method or a Gauss-Legendre collocation method. It should be noted that the local energy conservation law is admitted by more Hamiltonian PDEs than the multi-symplectic conservation law is. Hence our local energy-preserving methods can be more widely applied to multi-symplectic Hamiltonian PDEs than multi-symplectic methods in the literature. The numerical results accompanied in this paper are plausible and promising. In the experiments on CNLSs, our methods and the associated methods behave similarly to the multi-symplectic methods of the same order. In the experiments on 2DNLSs with external fields, our methods behave better than symplectic methods in both cubic and quintic nonlinear problems.

References

[1] N. Antar, N. Pamuk, Exact solutions of two dimensional nonlinear Schrödinger equations with external potentials, Appl. Comput. Math. 2 (2013) 152-158.

[2] T. J. Bridges, Multi-symplectic structures and wave propagation, Math. Proc. Camb. Philos. Soc. 121 (1997) 147-190.

[3] T. J. Bridges, S. Reich, Multi-symplectic integrators: numerical schemes for Hamiltonian PDEs than conserve symplecticity, Phys. Lett. A 284 (2001) 184-193.

[4] T. J. Bridges, S. Reich, Multi-symplectic spectral discretizations for the Zakhakarov-Kuznetsov and shallow water equations, Physica D 152-153 (2001) 491-504.

[5] T. J. Bridges, S. Reich, Numerical methods for Hamiltonian PDEs, J. Phys. A: Math. Gen. 39 (2006) 5287.

[6] J. Cai, Y. Wang, H. Liang, Local energy-preserving and momentum-preserving algorithms for coupled nonlinear Schrödinger system, J. Comput. Phys. 239 (2013) 30-50.

[7] J. Cai, Y. Wang, Local structure-preserving algorithms for the "good" Boussinesq equation, J. Comput. Phys. 239 (2013) 72-89.

[8] E. Celledoni, V. Grimm, R. I. Maclachlan, D. I. Maclaren, D. O'Neale, B. Owren, G. R. W. Quispel, Preserving energy resp. dissipation in numerical PDEs using the 'Average Vector Field' method, J. Comput. Phys. 231 (2012) 6770-6789.

[9] Y. Chen, Y. Sun, Y. Tang, Energy-preserving numerical methods for Landau-Lifshitz equation, J. Phys. A: Math. Theor. 44 (2011) 295207.

[10] Y. Chen, H. Zhu, S. Song, Multi-symplectic splitting method for the coupled nonlinear Schrödinger equation, Comput. Phys. Comm. 181 (2010) 1231-1241.

[11] J. B. Chen, M. Z. Qin, Multisymplectic Fourier pseudospectral method for the nonlinear Schrödinger equation, Electon. Trans. Numer. Anal. 12 (2001) 193-204.

[12] B. Deconinck, B. A. Frigyik, J. N. Kutz, Stability of exact solutions of the defocusing nonlinear Schrodinger equation with periodic potential in two dimensions, Phys. Lett. A 283 (2001) 177-184.

[13] Z. Fei, L. Vázquez, Two energy-conserving numerical schemes for the sine-Gordon equation, Appl. Math. Comput. 45 (1991) 17-30.

[14] Y. Gong, J. Cai, Y. Wang, Some new strcture-preserving algorithms for general multi-symplectic formulations of Hamiltonian PDEs, J. Comput. Phys. 279 (2014) 80-102.

[15] O. Gonzalez, Time Integration and Discrete Hamiltonian Systems, J. Nonlinear Sci. 6 (1996) 449-467.

[16] B. Y. Guo, L. Vázquez, A numerical scheme for nonlinear Klein–Gordon equation, J. Appl. Sci. 1 (1983) 25-32.

[17] E. Hairer, Energy-preserving variant of collocation methods, J. Numer. Anal. Ind. Appl. Math. 5 (2010) 73-84.

[18] J. Hong, X. Y. Liu, C. Li, The multi-symplecticity of partitioned Runge–Kutta methods for Hamiltonian PDEs, Math. Comput. 75 (2005) 167-181.

[19] J. Hong, X. Y. Liu, C. Li, Multi-symplectic Runge–Kutta–Nyström methods for Schrödinger equations with variable coefficients, J. Comput. Phys. 226 (2007) 1968-1984.

[20] A. L. Islas, C. M. Schober, C. Li, Backward error analysis for multisymplectic discretizations of Hamiltonian PDEs, Math. Comput. Simul. 69 (2005) 290-303.

[21] B. Karasözen, G. Simsek, Energy preserving integration of bi-Hamiltonian partial differential equations, TWMS. J. App. Eng. Math. 3 (2013) 75-86.

[22] L. Kong, J. Hong, F. Fu and J. Chen, Symplectic structure-preserving integrators for the two-dimensional Gross-Pitaevskii equation for BEC, J. Comput. Appl. Math. 235 (2011) 4937-4948.

[23] L. Kong, L. Wang, S. Jiang and Y. Duan, Multisymplectic Fourier pseudo-spectral integrators for Klein-Gordon-Schrödinger equations, Sci. China Math. 56 (2013) 915-932.

[24] S. Li, L. Vu-Quoc, Finite difference calculus invariant structure of a class of algorithms for the nonlinear Kelin-Gordon equation, SIAM J. Numer. Anal. 32 (1995) 1839-1875.

[25] R. I. Maclachlan, G. R. W Quispel, and N. Robidoux, Geometric Integration Using Dicrete Gradients, Philos. Trans. R. Soc. A 357 (1999) 1021-1046.

[26] R. I. Maclachlan, B. N. Ryland, and Y. Sun, High order multisymplectic Runge–Kutta methods, SIAM J. Sci. Comput. 36 (2014) A2199-A2226.

[27] J. E. Marsden, G. P. Patrick, and S. Shkoller, Multi-symplectic, variational integrators, and nonlinear PDEs, Comm. Math. Phys. 4 (1999) 351-395.

[28] B. E. Moore, S. Reich, Backward error analysis for multi-symplectic integration methods, Numerische Mathematik 95 (2003) 625-652.

[29] S. Reich, Multi-Symplectic Runge–Kutta Collocation Methods for Hamiltonian Wave Equation, J. Comput. Phys. 157 (2000) 473-499.

[30] B. N. Ryland, B. I. Maclachlan, J. Franco, On multi-symplecticity of partitioned Runge-Kutta and splitting methods, Int. J. Comput. Math. 84 (2007) 847-869.

[31] Y. Wang, B. Wang, M. Z. Qin, Local structure-preserving algorithms for partial differential equations, Science in China Series A: Mathematics, 51 (2008) 2115-2136.

[32] H. Zhu, S. Song, and Y. Tang, Multi-symplectic wavelet collocation method for the nonlinear Schrödinger equation and the Camassa-Holm equation, Comput. Phys. Comm. 182 (2011) 616-627.